Am J Transl Res 2025;17(4):2445-2466
www.ajtr.org /ISSN:1943-8141/AJTR0161425

Original Article

Downregulated TRAF3IP2-AS1 promotes hepatocellular carcinoma progression through the miR-374a-5p/SEL1L1/RPL6 axis to enhance DNA damage repair

Yu Wang[1,2*], Wen-Ze Wu[3*], Yuan-Wen Hu[4*], Qian-Qian Yu[5], Hai-Long Ge[2], Wei-Xin Yu[2], Feng Mo[2], Chen Chao[2], Dong-Lin Sun[1]

[1]Department of Hepatobiliary Surgery, The Third Affiliated Hospital of Soochow University, Changzhou 213003, Jiangsu, China; [2]Department of Hepatobiliary Surgery, Jintan Affiliated Hospital of Jiangsu University, Changzhou 213200, Jiangsu, China; [3]Department of General Surgery, The Affiliated Changzhou No. 2 People's Hospital of Nanjing Medical University, Changzhou 213003, Jiangsu, China; [4]Department of Gastroenterology, Kunshan First People's Hospital Affiliated to Jiangsu University, Kunshan 215300, Jiangsu, China; [5]Department of Oncology, Jintan Affiliated Hospital of Jiangsu University, Changzhou 213200, Jiangsu, China. [*]Equal contributors.

Received October 23, 2024; Accepted February 21, 2025; Epub April 15, 2025; Published April 30, 2025

Abstract: Objectives: Excessive activity in the DNA damage repair (DDR) pathway causes genomic instability, leading to the development of hepatocellular carcinoma (HCC), the most common form of liver cancer. The long non-coding RNA (lncRNA) tumor necrosis factor receptor-associated factor 3 interacting protein 2 antisense RNA 1 (TRAF3IP2-AS1) acts as a tumor suppressor. MicroRNA (miR)-374a-5p is a target miRNA for TRAF3IP2-AS1, while SEL1L ERAD E3 ligase adaptor subunit (SEL1L) acts as a target gene of miR-374a-5p. Moreover, DDR-participating molecule ribosomal protein L6 (RPL6) interacts with SEL1L. In this study, we aimed to explore the role and mechanism of TRAF3IP3-AS1 in HCC. Methods: In vitro HCC cell lines were cultured. In vivo, a mouse in situ HCC model was constructed using a liver injection of HepG2 cells. Additionally, clinical HCC and adjacent tissues were used to verify the pathway. Results: Oxidative stress downregulated TRAF3IP2-AS1 in HCC cells. TRAF3IP2-AS1 downregulated the proliferation, migration, and invasion of HCC cells by inhibiting miR-374a-5p levels. SEL1L was a target gene of miR-374a-5p in HCC cells. Mir-374a-5p facilitated the proliferation, migration, and invasion of HCC cells by inhibiting SEL1L. TRAF3IP2-AS1 and miR-374a-5p regulated the interaction between SEL1L and RPL6 as well as RPL6 ubiquitin degradation in HCC cells in an opposite manner. DDR was upregulated in HCC cells through the TRAF3IP2-AS1/miR-374a-5p/SEL1L1/RPL6 pathway. Downregulated SEL1L promoted the proliferation, migration, and invasion of HCC cells by upregulating RPL6 expression. Furthermore, the TRAF3IP2-AS1/miR-374a-5p/SEL1L/RPL6 pathway exacerbated the progression of HCC in mice. This pathway also promoted the proliferation, migration, and invasion of in vivo HCC cells by enhancing DDR. Conclusions: TRAF3IP2-AS1/miR-374a-5p/SEL1L/RPL6 pathway in HCC cells promoted DDR and HCC progression. Our data identify the role and mechanism of TRAF3IP2-AS1 in HCC and imply treatment targets for HCC.

Keywords: Tumor necrosis factor receptor-associated factor 3 interacting protein 2 antisense RNA 1 (TRAF3IP2-AS1), Hepatocellular carcinoma (HCC), MicroRNA (miR)-374a-5p, SEL1L ERAD E3 ligase adaptor subunit (SEL1L), Ribosomal protein L6 (RPL6), DNA damage repair (DDR)

Introduction

Liver cancer is the sixth most common cancer and the third most frequent cause of cancer-related death globally [1]. Hepatocellular carcinoma (HCC), the most common form of liver cancer, accounts for approximately 90% of all liver cancer cases [2]. The DNA damage repair (DDR) pathway is required when DNA genes are damaged, and it is indispensable for normal cell replication and metabolism. However, excessive activation of the DDR pathway can lead to genomic instability, leading to the development of HCC [3].

MicroRNAs (miRs) are a non-coding RNA with a length of approximately 22 nucleotides. They exist in a wide variety of different organisms,

https://doi.org/10.62347/UJZK5358

ranging from viruses to plants to humans. MiRs have many roles: specifically, they bind to the mRNA and recruit relevant RNases, leading to mRNA degradation and thereby blocking the expression of protein-coding genes and influencing their biological functions. Recent studies have revealed that miRs regulate the biological activities of HCC cells, including proliferation, invasion, metastasis, and epithelial-mesenchymal transition. Moreover, miR affects the metabolic processes, such as glycolysis, of HCC cells. For example, as an oncogene, miR-9 downregulates the expression of the p53 target gene p21, promoting the proliferation and invasion of HCC cells, thus contributing to the progression of HCC [4]. MiR-139-5p inhibits aerobic glycolysis, proliferation, migration, and invasion of HCC cells through reciprocal inhibitory effects with E26 transformation specific-1 [5]. In our study, we observed miR-374a-5p upregulation in human HCC tissues through miR sequencing results from the Gene Expression Omnibus (GEO) platform (GEO series number: GSE20594).

Long non-coding RNA (lncRNA), which is longer than 200 nt, acts on its downstream miR, affecting the expression and functions of miR. We focused on the tumor necrosis factor receptor-associated factor 3 interacting protein 2 antisense RNA 1 (TRAF3IP2-AS1), an upstream lncRNA of miR-374a-5p that is associated with tumors as determined through the starBase lncRNA-mir interaction database (website: http://starbase.sysu.edu.cn/starbase2/browseNcRNA.php). Downregulated TRAF3IP2-AS1 facilitates the progression of renal cell carcinoma [6]. In mouse psoriasis and autoimmune encephalomyelitis models (an animal model for multiple sclerosis), TRAF3IP2-AS1 promotes the production of the pro-inflammatory cytokine interleukin-17A [7].

We identified SEL1L ERAD E3 ligase adaptor subunit (SEL1L) as a target gene of miR-374a-5p through the MiRDB database (website: http://mirdb.org/cgi-bin/search.cgi?searchType=miRNA&searchBox=hsa-miR-374a-5p&full=1). SEL1L, which is highly conserved in various organisms, promotes the endoplasmic reticulum-associated degradation (ERAD) pathway by the ubiquitin-proteasome system. The ERAD pathway preserves cellular normal secretory function by recognizing and processing misfolded peptides for proteasome degradation. The overexpression of SEL1L can decrease the levels of hepatitis B virus (HBV) RNA, DNA, and cone and envelop proteins in hepatocytes. On the other hand, knockdown of SEL1L blocks the ERAD pathway, thereby activating the alternative endoplasmic reticulum quality control (ERQC)-autophagy pathway and leading to increased HBV RNA and cone protein levels [8]. Esophageal squamous cell carcinoma patients with a deficiency in the expression of SEL1L show a poor prognosis, indicating an anti-tumor effect of SEL1L [9]. Additionally, in non-small cell lung adenocarcinoma (NSCLA), the expression of SEL1L displays a negative correlation with the grade [10]. SEL1L inhibits pancreatic cancer cell proliferation *in vitro*, further affirming its tumor-suppressive role [11]. More importantly, SEL1L is expressed in hepatocytes [12], suppressing chemically induced hepatocyte proliferation and tumorigenesis in mice [13]. But several studies reveal an oncogenic role of SEL1L. For example, SEL1L immunoreactivity positively correlated with tumor progression and cell proliferation, and poor patient survival and response to therapy of human malignant gliomas [14].

Subsequently, using the Biological General Repository for Interaction Datasets (BioGRID) database (https://thebiogrid.org/112300), we found 85 kinds of proteins that interact with SEL1L. We focused on the ribosomal protein L6 (RPL6) among these proteins. RPL6 is a highly conserved ribosomal protein and acts as an essential component of the 50S subunit of ribosomes [15]. In response to DNA damage, RPL6 directly binds to histone H2A, and RPL6 silencing impairs DNA damage-induced H2A/H2AX ubiquitination and the interaction between MDC1 and gamma H2A histone family member X (γH2AX), leading to defects in DNA repair and reduced cell survival. RPL6 has been identified as a critical regulatory factor involved in DDR [16]. In addition, RPL6 plays a tumorigenesis role in multiple cancers, such as lung cancer [17], gastric cancer [18], and gallbladder carcinoma [19].

In this study, we investigated the effect of the TRAF3IP2-AS1/miR-374a-5p/SEL1L1/RPL6 pathway on the progression of HCC through the DDR mechanism. We cultured HCC cell lines in vitro. *In vivo*, a mouse in situ HCC model was created by injecting HepG2 cells into the liver. Additionally, clinical HCC and adjacent tissues

were used to verify the pathway. Our study aims to discover a novel regulation mechanism of DDR during HCC, thus supplying candidate molecular targets for the treatment of HCC.

Materials and methods

Tissue samples

A total of 20 pairs of HCC tissues and matched para-HCC tissues were collected from HCC patients at Jintan Hospital (Jiangsu, China), with written informed consent. Preoperative chemotherapy or radiotherapy was administered to each of the patients in this study.

Cell culture and treatment

L02 cells (CRL-12461) purchased from the American Type Culture Collection (ATCC) as well as HepG2 (SCSP-510) and Huh7 (SCSP-526) cells purchased from the Chinese Academy of Sciences Cell Bank were cultured in Dulbecco's Modified Eagle Medium (DMEM; 11965092, Gibco, USA) supplemented with 10% fetal bovine serum (FBS; 10091, Thermo Fisher Scientific, USA) at 37°C and under 5% CO_2. The cells were treated with 0.1% dimethyl sulfoxide (DMSO; 67-68-5, Sigma Aldrich, USA; 10 μL) for 24 h, hydrogen peroxide (H_2O_2; an oxidative stress inducer; 31642, Sigma Aldrich; 200 μM) for 24 h, and H_2O_2 + resveratrol (RSV; an antioxidant; 501-36-0, Sigma Aldrich; 10 μM) for 24 h.

Plasmid construction and transfection

The human TRAF3IP2-AS1 sequence was synthesized by GeneChem Technology (China) and subcloned into the hemagglutinin (HA)-tag vector (55182, Addgene, USA). The human RPL6 cDNA ORF Clone (HG17086-UT, SinoBiological, USA) was subcloned into the Flag-tag vector (55180, Addgene). The SEL1L3'-3'-untranslated region (UTR) wild type (WT) or pmirGLO-SEL1L3'-UTR mutant (sequences can be found in **Figure 3E**) was subcloned (GeneChem Technology) into pmirGLO (VT1439, YouBio, China). The cells were transfected through HA-tag (empty vector; 40 μg), HA-TRAF3IP2-AS1 (TRAF3IP2; 40 μg), TRAF3IP2 siRNA (TRAF3IP2-AS1 inhibitor; 4390771, Thermo Fisher Scientific, USA; 10 nM), miR-374a-5p mimics (HY-R00829, MedChemExpress, USA; 50 nM), miR-374a-5p inhibitor (AM17000, Thermo Fisher Scientific; 100 nM), SEL1L siRNA (SR304313, Origene; 10 nM), pcDNA3.1-SEL1L (OHu19523, GenScript, USA; 1 μg), RPL6 siRNA (AM16708, Thermo Fisher Scientific; 10 nM), Flag-RPL6 (1 μg), miR-374a-5p mimics NC (4464058, Thermo Fisher Scientific; 50 nM), pmirGLO-SEL1L3'-untranslated region (UTR) wild type (WT; 1 μg), or pmirGLO-SEL1L3'-UTR MUT (1 μg), using Lipofectamine 2000 (11668019, Thermo Fisher Scientific). The transfection lasted for 24 h, after which subsequent experiments were performed.

RNA isolation and quantitative real-time polymerase chain reaction (qRT-PCR)

Total RNA was extracted from human HCC, para-HCC tissues, L02, HepG2 cells, Huh7 cells, or mouse liver tissues using TRIzol (15596026). Then, 1 mg of total RNA for each sample was reverse-transcribed using the SuperScript II Reverse Transcriptase (18064-022). The resulting cDNA was subjected to qRT-PCR using SYBR Green Real-Time PCR Master Mix (4309155). All the reagents used for RNA isolation and qRT-PCR were purchased from Thermo Fisher Scientific. All gene expression results were expressed as arbitrary units relative to the expression of GAPDH. The primer sequences used were as follows: 1. TRAF3IP2-AS1 forward: 5'-TTTGGCGGCTATGCAGGATT-3' and reverse: 5'-TGTCCATGTGGTATTGGGCA-3' [6]. 2. miR-374a-5p forward: 5'-GCGCGCTTATAATACAACCTGA-3' and reverse: 5'-GTGCAGGGTCCGAGGT-3' [20].

Cell proliferation assay

The proliferation of HepG2 and Huh7 cells was assessed using the 5-ethynyl-2'-deoxyuridine (EdU) cell proliferation assay with the Cell-LightTM Cell-Light EdU Apollo567 In Vitro Kit (C10310-1, Guangzhou RiboBio, China). Briefly, HepG2 or Huh7 cells (1×10^4) were seeded in each well of 96-well plates for transfection. After incubation at 37°C and under 5% CO_2 for 24 h, the cells were treated with 50 mM EdU and incubated for an additional 2 h. The cells were then fixed with 4% paraformaldehyde (PFA) and stained with ApolloH Dye Solution to detect proliferating cells. All the cell nuclei were stained with DAPI (C1002, Beyotime, China). Images were captured using a fluorescence microscope (Olympus, Japan).

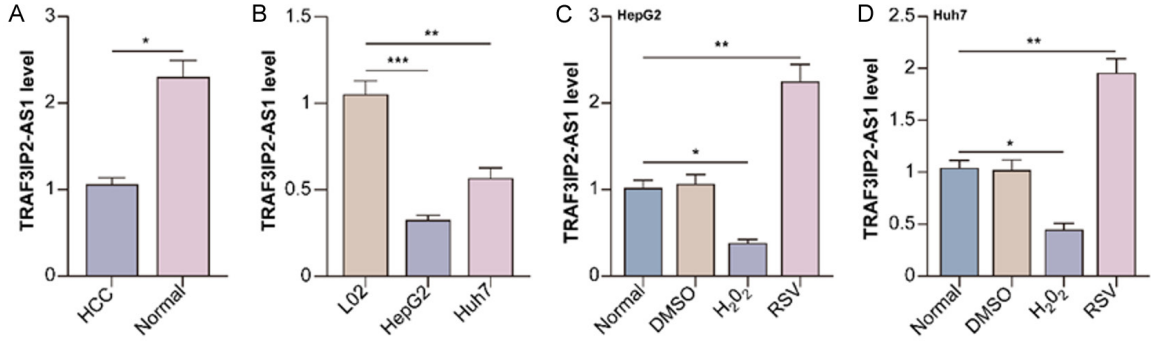

Figure 1. Oxidative stress downregulates tumor necrosis factor receptor-associated factor 3 interacting protein 2 antisense RNA 1 (TRAF3IP2-AS1) in HCC cells. A: TRAF3IP2-AS1 levels in human hepatocellular carcinoma (HCC) and adjacent tissues were evaluated through quantitative real-time polymerase chain reaction (qRT-PCR). $^{*}P < 0.05$ vs. the para-HCC group. B: TRAF3IP2-AS1 levels in L02, HepG2, and Huh7 cells were detected through qRT-PCR. $^{**}P < 0.01$ and $^{***}P < 0.001$ vs. the L02 cell group. HepG2 and Huh7 cells were divided into normal, 0.1% dimethyl sulfoxide (DMSO) (10 μL for 24 h), hydrogen peroxide (H_2O_2) (200 μM for 24 h), and H_2O_2 + resveratrol (RSV) (10 μM for 24 h) groups. C: TRAF3IP2-AS1 levels in HepG2 cells were evaluated using qRT-PCR. $^{*}P < 0.05$ and $^{**}P < 0.01$ vs. the HepG2 cell normal group. D: TRAF3IP2-AS1 levels in Huh7 cells were evaluated through qRT-PCR. $^{*}P < 0.05$ and $^{**}P < 0.01$ vs. the Huh7 cell normal group.

Transwell migration assay

Transwell chambers with 8 μm pores for 24-well plates (3422, Corning, USA) were prepared. HepG2 or Huh7 cells were seeded into the upper chambers at a density of 1×10^4 cells/well, while the lower chambers were filled with a 600 μL medium containing 10% FBS. The cells were treated differently for 24 h. Then, the cells that migrated to the lower chambers were fixed with 4% PFA and stained with 0.5% crystal violet (C0121, Beyotime) before counting using an inverted microscope 24 h later.

Transwell Matrigel invasion assays

Matrigel (10 mg/mL; 356234, Corning) was left at 4°C and melted overnight, and then diluted 6 times with DMEM. Sixty microliters of diluted Matrigel were added to the upper chamber of an 8 μm Transwell for a 24-well plate. After incubation at 37°C for 2 h, the Matrigel solidified. HepG2 cells were seeded in the upper chamber of the Transwell at a density of 1×10^4 cells/well using serum-free DMEM. Five hundred microliters of DMEM with 10% FBS were added to the lower chamber of Transwell. After 24 h, the chambers were fixed with 4% PFA and stained with 0.5% crystal violet.

Western blot

Proteins (50 μg/lane) were separated through sodium dodecyl sulfate-polyacrylamide gel electrophoresis (SDS-AGE) and transferred onto polyvinylidene difluoride (PVDF) membranes [21]. The membranes were blocked in 5% nonfat dried milk for 1 h at room temperature. The membranes were subsequently incubated with a specific primary antibody overnight at 4°C and then incubated with a corresponding horseradish peroxidase (HRP)-conjugated secondary antibody for 1 h at room temperature. The primary antibodies were as follows: mouse anti-SEL1L (sc-377350, Santa Cruz Biotechnology, USA; 1 μg/ml); mouse anti-p-ataxia telangiectasia mutation (ATM; Ser1981; MA1-2020, Thermo Fisher Scientific; 1:500); rabbit anti-ATM (MA5-32063, Thermo Fisher Scientific; 1:2000); rabbit anti-γH2AX (Ser139; 2595, Cell Signaling Technology, USA; 1:1000); rabbit anti-RPL6 (PA5-30217, Thermo Fisher Scientific; 1:4000); mouse anti-GAPDH (sc-47724, Santa Cruz Biotechnology; 0.5 μg/ml); mouse anti-β-actin (sc-47778, Santa Cruz Biotechnology; 0.5 μg/ml).

The secondary antibodies used were HRP-conjugated goat anti-mouse IgG (SA00001-1, Proteintech, USA; 1:4000) and HRP-conjugated goat anti-rabbit IgG (SA00001-2, Proteintech; 1:4000). After each incubation, PBS was washed 3 times. Finally, the proteins were visualized using enhanced chemiluminescent reagents (34580; Thermo Fisher Scientific).

Luciferase reporter assay

After 24 h of transfection, HepG2 or Huh7 cells were harvested and assayed using a dual-lucif-

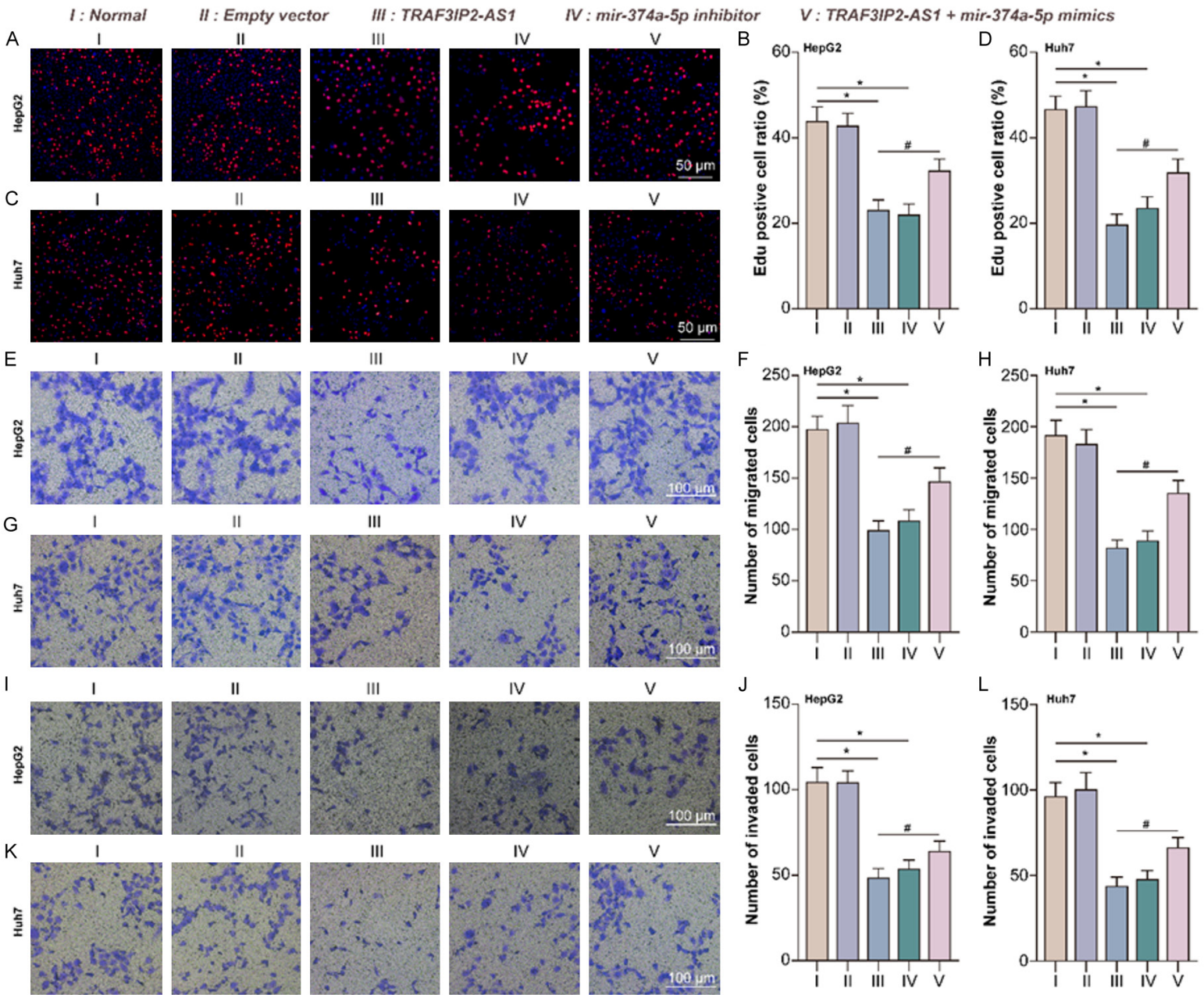
I : Normal
II : Empty vector
III : TRAF3IP2-AS1
IV : mir-374a-5p inhibitor
V : TRAF3IP2-AS1 + mir-374a-5p mimics
A
B
C
D
E
F
G
H
I
J
K
L
HepG2
Huh7
50 μm
100 μm
Edu postive cell ratio (%)
Number of migrated cells
Number of invaded cells

Figure 2. TRAF3IP2-AS1 downregulates the proliferation, migration, and invasion of HCC cells by inhibiting microRNA (miR)-374a-5p levels. HepG2 and Huh7 cells were divided into the normal, empty vector, TRAF3IP2-AS1, miR-374a-5p inhibitor, and TRAF3IP2-AS1 + miR-374a-5p mimics groups. Each vector or sequence was transfected for 24 h. (A) HepG2 cell proliferation was determined through a 5-ethynyl-2'-deoxyuridine (EdU) assay. (B) The ratio of EdU-positive HepG2 cell number to DAPI-positive HepG2 cell number was analyzed. (C) Huh7 cell proliferation was detected using the EdU assay. (D) The ratio of EdU-positive Huh7 cells to DAPI-positive Huh7 cells was analyzed. (E) The migration of HepG2 cells was detected through a Transwell assay. (F) The number of migrated HepG2 cells was analyzed. (G) The migration of Huh7 cells was detected through the Transwell assay. (H) The number of migrated Huh7 cells was analyzed. (I) The invasion of HepG2 cells was detected using the Matrigel Transwell assay. (J) The number of invaded HepG2 cells was analyzed. (K) The invasion of Huh7 cells was detected using the Matrigel Transwell assay. (L) The number of invaded Huh7 cells was analyzed. In (B, F, J), $^{*}P < 0.05$ vs. the HepG2 cell normal group. $^{\#}P < 0.05$ vs. the HepG2 cell TRAF3IP2-AS1 group. In (D, H, L), $^{*}P < 0.05$ vs. the Huh7 cell normal group. $^{\#}P < 0.05$ vs. the Huh7 cell TRAF3IP2-AS1 group.

erase reporter assay system (E1910; Promega, USA).

Chromatin immunoprecipitation (ChIP)

ChIP was performed using a magnetic ChIP kit (26157; Thermo Fisher Scientific). In brief, 80% of confluent HepG2 or Huh7 cells were cross-linked with formaldehyde to a final concentration of 1%. The cells were lysed using SDS lysis buffer and sonicated to shear DNA to 200-500 base pair fragments. Subsequently, the DNA fragments were immunoprecipitated overnight with 10 μg of anti-SEL1L antibody per reaction. Purified and eluted DNA fragments were then quantified using real-time PCR.

Immunoprecipitation (IP)

For IP, HepG2 or Huh7 cells were transfected with HA-Ubiquitin (Ub) (18712; Addgene; 1 μg) and lysed in IP buffer supplemented with a protease inhibitor cocktail (ab271306; Abcam, USA). Then the cell lysates were incubated overnight at 4°C with RPL6 or SEL1L antibody at a 1:100 dilution along with Protein G agarose beads (sc-2002; Santa Cruz Biotechnology) as previously described [22]. The immunoprecipitants were enriched and denatured at 100°C for 10 min in a 2 × SDS-PAGE loading buffer. The inputs and immunoprecipitants were then subjected to western blot (WB) analysis.

Cycloheximide (CHX) chase assay

To determine the change of RPL6 stability in HepG2 or Huh7 cells, a CHX chase assay was performed. In brief, the cells were treated with CHX (HY-12320, MedChemExpress; 20 pg/ml for 24 h) to inhibit protein synthesis. The expression of RPL6 was analyzed using western blotting with corresponding antibodies.

Mouse xenograft model of HepG2 cells

All animal experiments were performed in accordance with replacement, reduction, and refinement principles to minimize animal suffering. A total of 63 male BALB/c nude mice, aged 5-6 weeks and weighing 16 ± 2 g, were purchased from the Laboratory Animal Center of Soochow University. The prepared HepG2 cells (approximately 2×10^6 cells in 200 μL) were injected subcutaneously on the back of each nude mouse. The tumor size of the mouse was assessed daily using a vernier caliper. The tumor volume was calculated using the formula: tumor size = length × $(\text{width})^2/2$.

Mouse serum alpha-fetoprotein (AFP) detection

Serum was prepared from mouse blood samples by centrifugation, and AFP in mouse serum was tested using an enzyme-linked immunosorbent assay (ELISA) kit (MAFP00, R&D Systems, USA).

Immunohistochemistry (IHC)

HCC or mouse tumor tissues were fixed in 10% formalin and embedded in paraffin. Next, 4 μm-thick consecutive sections were cut and mounted on glass slides. After deparaffinization, antigen retrieval was done on the tissue sections, and then they were washed and treated with a peroxidase-blocking solution (Santa Cruz). Then, the sections were incubated with mouse anti-SEL1L (1:50), rabbit anti-RPL6 (1:500), mouse anti-proliferating cell nuclear antigen (PCNA; ab29, Abcam; 1:10000), mouse anti-F-actin (ab205, Abcam; 1:5000), or mouse anti-β1-integrin antibody (sc-9970, Santa Cruz Biotechnology; 1:50). After washing with PBS, the sections were incubated with a biotinylated goat anti-mouse IgG (31800, Thermo Fisher

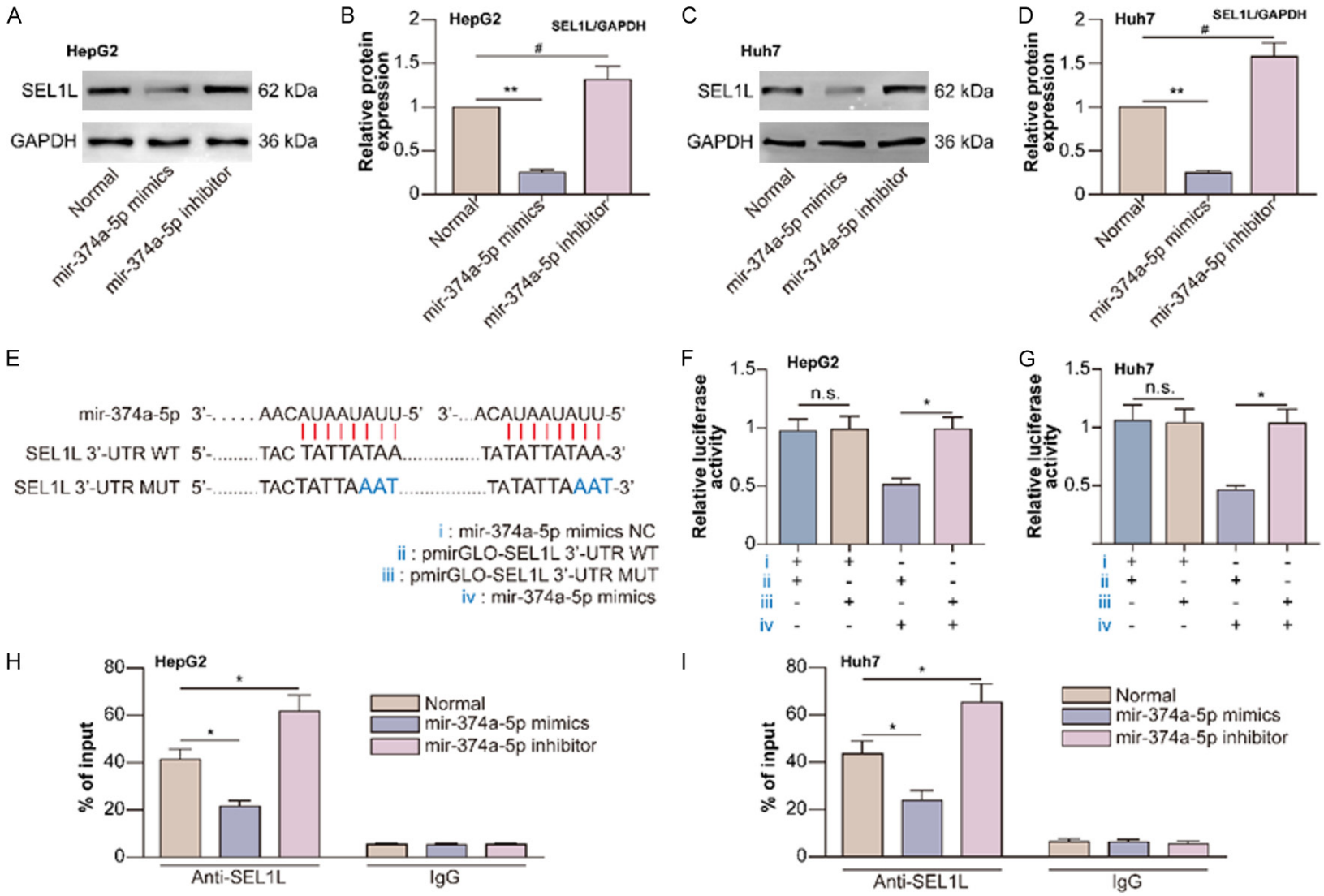

Figure 3. SEL1L ERAD E3 ligase adaptor subunit (SEL1L) is the target gene of miR-374a-5p in HCC cells. HepG2 and Huh7 cells were divided into the normal, miR-374a-5p mimics, and miR-374a-5p inhibitor groups. A: SEL1L protein levels in HepG2 cells were detected using western blot (WB). B: SEL1L protein levels in HepG2 cells were analyzed. $^{**}P < 0.01$ the HepG2 cell miR-374a-5p mimics group vs. the HepG2 cell normal group. $^{\#}P < 0.05$ the HepG2 cell miR-374a-5p inhibitor group vs. the HepG2 cell normal group. C: SEL1L protein levels in Huh7 cells were determined through WB. D: SEL1L protein levels in Huh7 cells were analyzed. $^{**}P < 0.01$ the

Huh7 cell miR-374a-5p mimics group vs. the Huh7 cell normal group. #*P* < 0.05 the Huh7 cell miR-374a-5p inhibitor group vs. the Huh7 cell normal group. E: The binding sequence between miR-374a-5p and the untranslated region (UTR) of SEL1L mRNA. HepG2 and Huh7 cells were divided into miR-374a-5p mimics NC + pmirGLO-SEL1L3'-UTR wild type (WT), miR-374a-5p mimics NC + pmirGLO-SEL1L3'-UTR MUT, miR-374a-5p mimics + pmirGLO-SEL1L3'-UTR WT, and miR-374a-5p mimics + pmirGLO-SEL1L3'-UTR MUT groups. F: The activity of SEL1L promoter in HepG2 cells was determined through a luciferase reporter assay. "n.s." indicates no significance compared to the HepG2 cell miR-374a-5p mimics NC + pmirGLO-SEL1L3'-UTR WT group. **P* < 0.05 vs. the HepG2 cell miR-374a-5p mimics + pmirGLO-SEL1L3'-UTR MUT groups. G: The activity of SEL1L promoter in Huh7 cells was determined through a luciferase reporter assay. "n.s." vs. Huh7 cell miR-374a-5p mimics NC + pmirGLO-SEL1L3'-UTR MUT group. **P* < 0.05 vs. Huh7 cell miR-374a-5p mimics + pmirGLO-SEL1L3'-UTR WT groups. HepG2 and Huh7 cells were divided into input, IgG, and anti-SEL1L groups with or without miR-374a-5p mimics and miR-374a-5p inhibitor transfection. The results are represented by the ratio to the input signal. H: Chromatin immunoprecipitation (ChIP) in HepG2 cells was followed by qRT-PCR for miR-374a-5p. **P* < 0.05 vs. the HepG2 cell normal anti-SEL1L antibody group. I: ChIP in Huh7 cells was followed by qRT-PCR for miR-374a-5p. **P* < 0.05 vs. the Huh7 cell normal anti-SEL1L antibody group.

Scientific; 1:2000), biotinylated goat anti-rabbit IgG (65-6140, Thermo Fisher Scientific; 1:8000), and HRP-streptavidin complex (ab-64269, Abcam). The color was developed using a diaminobenzidine substrate. All sections were counterstained with diluted hematoxylin.

Statistical analysis

All the values were presented as mean ± standard error of the mean (SEM) of at least three independent experiments. SPSS 20.0 software package was used for statistical analyses. A two-sided t-test was used for comparisons of two groups, while a one-way ANOVA with Tukey's post hoc test was used for all other variables. *P* < 0.05 was considered significant.

Results

Oxidative stress downregulates TRAF3IP2-AS1 in HCC cells

According to the GEO database (GSE49515), TRAF3IP2-AS1 levels in peripheral blood mononuclear cells of HCC patients were found to be lower than those in normal controls. TRAF3IP2-AS1 decreased in HCC tissues compared to adjacent tissues (**Figure 1A**). Similarly, TRAF3IP2-AS1 was lower in HepG2 and Huh7 cells than it was in L02 cells (**Figure 1B**). Mounting evidence has revealed that oxidative stress (OS) in hepatocytes is associated with the development of HCC [23]. Under OS, Keap1 regulation-associated lncRNA (KRAL) is downregulated in HCC cells [24]. Therefore, the effect of OS on TRAF3IP2-AS1 was investigated. In both HepG2 (**Figure 1C**) and Huh7 (**Figure 1D**) cells, the TRAF3IP2-AS1 level decreased when treated with H_2O_2 and increased when treated with RSV (an antioxidant reagent), indicating that OS in HCC cells downregulates TRAF3IP2-AS1.

TRAF3IP2-AS1 downregulates the proliferation, migration, and invasion of HCC cells by inhibiting miR-374a-5p levels

The downstream miR-374a-5p levels of TRAF3IP2-AS1 in HCC tissues were higher than in adjacent tissues (Figure S1A). Similarly, MiR-374a-5p levels were higher in HepG2 and Huh7 cells than in analogous L02 cells (Figure S1B). The interaction sites between miR-374a-5p and TRAF3IP2-AS1 were obtained from the starBase lncRNA-mir interaction database (Figure S2A). In HepG2 (Figure S2B) and Huh7 (Figure S2C) cells, TRAF3IP2-AS1 decreased mir-374-5p levels, suggesting that TRAF3IP2-AS1 downregulates miR-374a-5p. TRAF3IP2-AS1 decreased the EdU-positive cell ratio (**Figure 2A-D**), migrated cell number (**Figure 2E-H**), and invaded cell number (**Figure 2I-L**) of HepG2 and Huh7 cells, while miR-374a-5p mimics partly reversed the effects of TRAF3IP2-AS1. At the same time, the miR-374a-5p inhibitor showed similar effects as TRAF3IP2-AS1.

SEL1L is the target gene of miR-374a-5p in HCC cells

The target gene of miR-374a-5p was identified as SEL1L, whose expression was positively correlated to the total survival time of HCC patients (Figure S3A). SEL1L expression was lower in HCC tissues than in adjacent tissues, as determined through IHC (Figure S3B) and WB (Figure S3C, S3D). Additionally, SEL1L expression in HepG2 and Huh7 cells was weaker than in L02 cells (Figure S3E, S3F). In HepG2 (**Figure 3A**, **3B**) and Huh7 (**Figure 3C**, **3D**) cells, SEL1L expression was decreased by miR-374a-5p mimics and increased by the miR-374a-5p inhibitor. Additionally, SEL1L3'-UTR WT and SEL1L3'-UTR MUT (**Figure 3E**) luciferase plasmids were constructed and transfected. MiR-

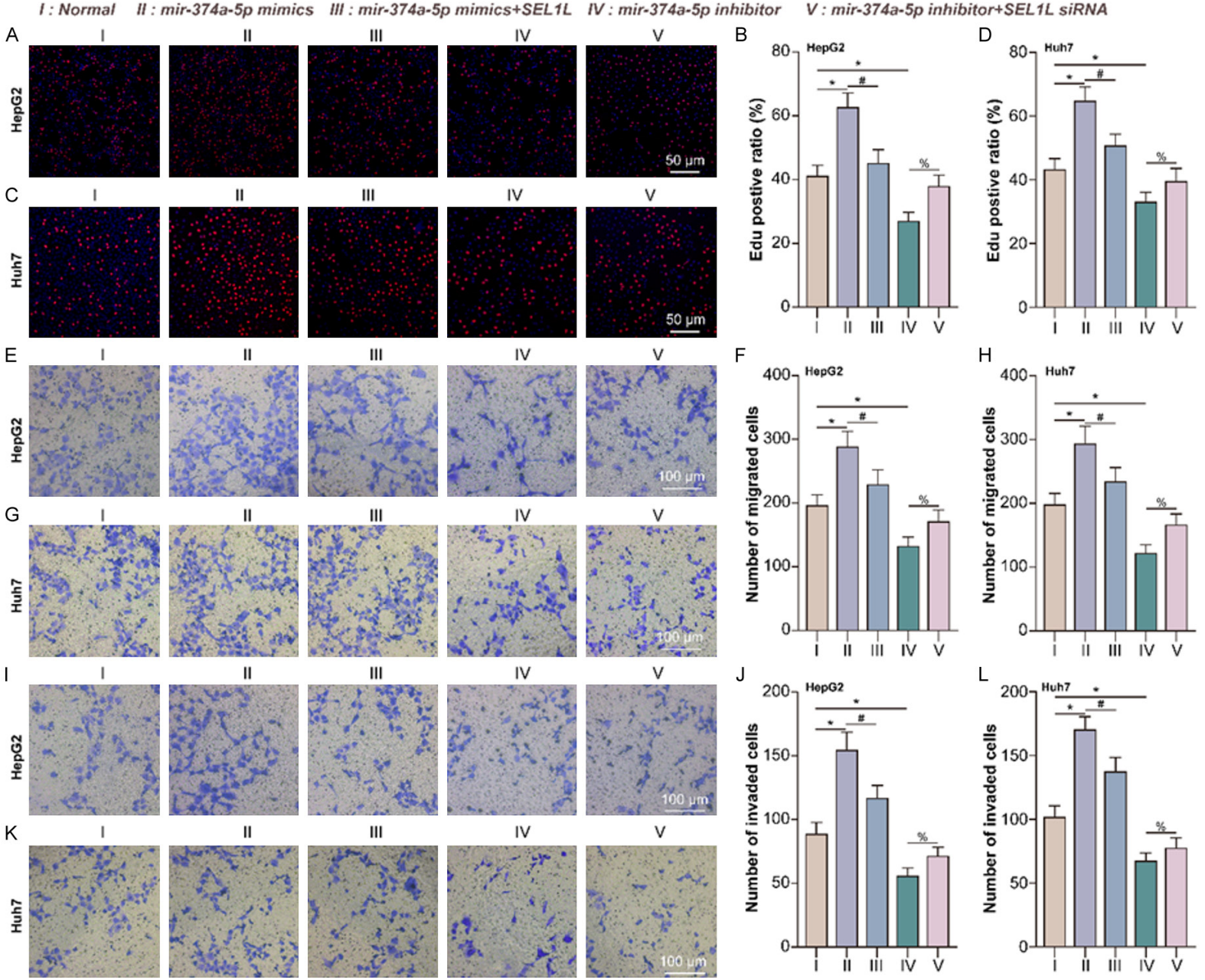
I : Normal
II : mir-374a-5p mimics
III : mir-374a-5p mimics+SEL1L
IV : mir-374a-5p inhibitor
V : mir-374a-5p inhibitor+SEL1L siRNA
A
B
C
D
E
F
G
H
I
J
K
L
HepG2
Huh7
50 μm
100 μm
Edu postive ratio (%)
Number of migrated cells
Number of invaded cells

Figure 4. MiR-374a-5p facilitates the proliferation, migration, and invasion of HCC cells by inhibiting SEL1L. HepG2 and Huh7 cells were divided into normal, miR-374a-5p mimics, miR-374a-5p mimics + SEL1L CRISPR activation plasmid (sc-403861-ACT, Santa Cruz Biotechnology), miR-374a-5p inhibitor, and miR-374a-5p inhibitor + SEL1L siRNA groups. (A) HepG2 cell proliferation was determined through an EdU assay. (B) The ratio of EdU-positive HepG2 cells to DAPI-positive HepG2 cells was analyzed. (C) Huh7 cell proliferation was determined through an EdU assay. (D) The ratio of EdU-positive Huh7 cells to DAPI-positive Huh7 cells was analyzed. (E) The migration of HepG2 cells was determined through a Transwell assay. (F) The number of migrated HepG2 cells was analyzed. (G) The migration of Huh7 cells was determined through a Transwell assay. (H) The number of migrated Huh7 cells was analyzed. (I) The invasion of HepG2 cells was determined through a Matrigel Transwell assay. (J) The number of invaded HepG2 cells was analyzed. (K) The invasion of Huh7 cells was determined through a Matrigel Transwell assay. (L) The number of invaded Huh7 cells was analyzed. In (B, F, J), $^{*}P < 0.05$ vs. the HepG2 cell normal group. $^{\#}P < 0.05$ vs. the HepG2 cell miR-374a-5p mimics group. $^{\%}P < 0.05$ vs. the HepG2 cell miR-374a-5p inhibitor group. In (D, H, L), $^{*}P < 0.05$ vs. the Huh7 cell normal group. $^{\#}P < 0.05$ vs. Huh7 cell miR-374a-5p mimics group. $^{\%}P < 0.05$ vs. the Huh7 cell miR-374a-5p inhibitor group.

374a-5p mimics, rather than miR-374a-5p mimics NC, decreased SEL1L 3'-UTR WT transcription activity compared to that of SEL1L 3'-UTR MUT in HepG2 (**Figure 3F**) and Huh7 (**Figure 3G**) cells. Interestingly, miR-374a-5p mimics decreased the binding between miR-374a-5p and SEL1L 3'-UTR in HepG2 (**Figure 3H**) and Huh7 (**Figure 3I**) cells, while the miR-374a-5p inhibitor increased this binding. These results may be due to the negative regulatory role of miR-374a-5p on SEL1L mRNA. Mir-374a-5p decreased SEL1L mRNA, including SEL1L 3'-UTR, leading to decreased binding of SEL1L 3'-UTR to miR-374a-5p.

MiR-374a-5p facilitates the proliferation, migration, and invasion of HCC cells by inhibiting SEL1L

The EdU-positive cell ratio, migrated cell number, and invaded cell number for HepG2 and Huh7 cells were increased by miR-374a-5p mimics, while co-treatment with SEL1L overexpression partly reversed the effects of miR-374a-5p mimics. In addition, the miR-374a-5p inhibitor decreased the EdU-positive cell ratio (**Figure 4A-D**), migrated cell number (**Figure 4E-H**), and invaded cell number (**Figure 4I-L**) for HepG2 and Huh7 cells, which were partly reversed by co-treatment with SEL1L knockdown.

TRAF3IP2-AS1 and miR-374a-5p regulate the interaction between SEL1L and RPL6 as well as RPL6 ubiquitin degradation in HCC cells in opposite directions

We observed that RPL6, an interacting protein of SEL1L, was negatively correlated to the total survival time of HCC patients (Figure S4A). RPL6 expression was higher in HCC tissues compared to adjacent tissues, as determined by IHC (Figure S4B) and WB (Figure S4C, S4D). Moreover, RPL6 expression was higher in HepG2 and Huh7 cells than it was in L02 cells (Figure S4E, S4F). We investigated the effect of the TRAF3IP2-AS1/miR-374a-5p/SEL1L pathway on RPL6. In HepG2 (Figure S5A, S5B) and Huh7 (Figure S5C, S5D) cells, RPL6 expression was decreased by TRAF3IP2-AS1 overexpression, miR-374a-5p inhibitor, or SEL1L overexpression, indicating that the TRAF3IP2-AS1/miR-374a-5p/SEL1L pathway upregulated RPL6 expression in HCC cells. In L02 cells, TRAF3IP2-AS1 overexpression, the miR-374a-5p inhibitor, or SEL1L overexpression had no effect on the interaction between SEL1L and RPL6 (**Figure 5A** and **5B**). However, in HepG2 (**Figure 5C** and **5D**) and Huh7 (**Figure 5E** and **5F**) cells, the interaction between SEL1L and RPL6 was upregulated by TRAF3IP2-AS1 overexpression, the miR-374a-5p inhibitor, or SEL1L overexpression. These findings reveal that the TRAF3IP2-AS1/miR-374a-5p/SEL1L pathway downregulated the interaction between RPL6 and SEL1L in HCC cells but not in normal human hepatocytes. Moreover, the ubiquitination of RPL6 in HepG2 (**Figure 5G**) and Huh7 (**Figure 5H**) cells was upregulated by TRAF3IP2-AS1 overexpression, the miR-374a-5p inhibitor, or SEL1L overexpression. Furthermore, the half-life of RPL6 in HepG2 (Figure S6A and S6B) and Huh7 (Figure S6C and S6D) cells was reduced by TRAF3IP2-AS1 overexpression, the miR-374a-5p inhibitor, or SEL1L overexpression. Therefore, we speculated that the TRAF3IP2-AS1/miR-374a-5p/SEL1L pathway downregulated the interaction between SEL1L and RPL, thereby inhibiting the ubiquitin degradation of RPL6 in HCC cells.

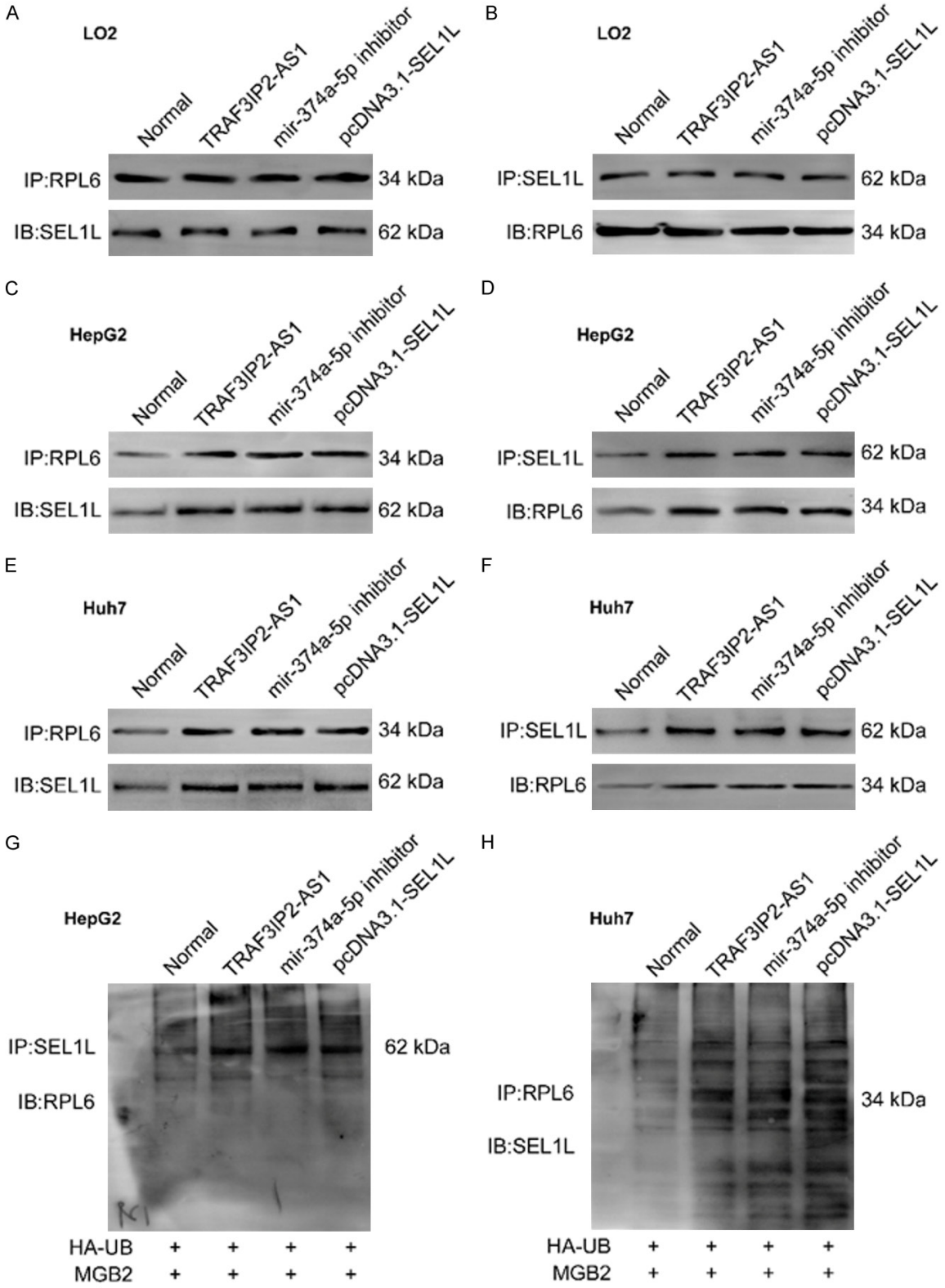

Figure 5. TRAF3IP2-AS1 and miR-374a-5p regulate the interaction between SEL1L and ribosomal protein L6 (RPL6) as well as RPL6 ubiquitin degradation in HCC cells in an opposing manner. L02, HepG2, and Huh7 cells were divided into normal, TRAF3IP2-AS1, miR-374a-5p inhibitor, and pcDNA3.1-SEL1L groups. A: The interaction between SEL1L and RPL6 in L02 cells was evaluated by IP using the anti-SEL1L antibody. B: The interaction between SEL1L

and RPL6 in L02 cells was evaluated through IP using the anti-RPL6 antibody. C: The interaction between SEL1L and RPL6 in HepG2 cells was determined by Co-immunoprecipitation (CO-IP) using the anti-SEL1L antibody. D: The interaction between SEL1L and RPL6 in HepG2 cells was determined by CO-IP using the anti-RPL6 antibody. E: The interaction between SEL1L and RPL6 in Huh7 cells was determined by IP using the anti-SEL1L antibody. F: The interaction between SEL1L and RPL6 in Huh7 cells was determined by CO-IP using the anti-RPL6 antibody. HepG2 and Huh7 cells were divided into hemagglutinin (HA)-Ubiquitin (Ub) + MG132, HA-Ub + MG132 + TRAF3IP2-AS1, HA-Ub + MG132 + miR-374a-5p inhibitor, and HA-Ub + MG132 + pcDNA3.1-SEL1L groups. G: The ubiquitination levels of RPL6 in HepG2 cells were detected by IP using the anti-HA antibody. H: The ubiquitination levels of RPL6 in Huh7 cells were determined by IP using the anti-HA antibody.

DDR is upregulated in HCC cells by the TRAF3IP2-AS1/miR-374a-5p/SEL1L1/RPL6 pathway

During DDR, ATM is activated through its phosphorylation on S1981. Then activated ATM phosphorylates one of the variants of histone H2AX - histone H2AX on Ser139 (γH2AX) - that is not only a major participant but also an early marker of cellular response to DNA damage [25]. In HepG2 (**Figure 6A-D**) and Huh7 (**Figure 6E-H**) cells, p-ATM, ATM, and γH2AX expression was decreased by TRAF3IP2-AS1 overexpression, the miR-374a-5p inhibitor, SEL1L overexpression, or RPL6 knockdown.

Downregulated SEL1L promotes the proliferation, migration, and invasion of HCC cells by promoting RPL6 expression

We investigated the roles of the SEL1L/RPL6 pathway in the biological behaviors of HCC cells. EdU-positive cell ratio (**Figure 7A-D**), migrated cell number (**Figure 7E-H**), and invaded cell number (**Figure 7I-L**) of HepG2 and Huh7 cells were decreased by RPL6 knockdown or SEL1L overexpression, but SEL1L overexpression with RPL6 overexpression partly counteracted the influence of SEL1L overexpression.

The TRAF3IP2-AS1/miR-374a-5p/SEL1L/RPL6 pathway exacerbates the progression of HCC in mice

To further validate the expression and role of the TRAF3IP2-AS1/miR-374a-5p/SEL1L/RPL6 pathway in HCC, an *in situ* HCC mouse model was established by injecting HepG2 cells into the skin for 28 d. The expression of TRAF3IP2-AS1 was lower (**Figure 8A**), while that of miR-374a-5p was higher (**Figure 8B**) in mouse HCC tissues than in adjacent tissues. Furthermore, SEL1L expression decreased while RPL6 expression increased (**Figure 8C-E**) in mouse HCC tissues relative to adjacent tissues. Additionally, tumor volume (**Figure 8F**), tumor weight (**Figure 8G**), and serum AFP (**Figure 8H**) were decreased by TRAF-AS1 overexpression, the miR-374a-5p inhibitor, SEL1L overexpression, or RPL6 knockdown.

The TRAF3IP2-AS1/miR-374a-5p/SEL1L/RPL6 pathway promotes the proliferation, migration, and invasion of in vivo HepG2 cells by promoting DDR

The expression of DDR markers p-ATM, ATM, and γH2AX increased in mouse HCC tissues compared to adjacent tissues (**Figure 9A-D**). However, TRAF-AS1 overexpression, the miR-374a-5p inhibitor, SEL1L overexpression, or RPL6 knockdown decreased p-ATM, ATM, and γH2AX expression in mouse HCC tissues (**Figure 9E-H**). In addition, TRAF-AS1 overexpression, the miR-374a-5p inhibitor, SEL1L overexpression, or RPL6 knockdown decreased the reactivity of PCNA (a cell proliferation marker; **Figure 9I**), F-actin (a cell migration marker; **Figure 9J**), and β1-integrin (a cell invasion marker; **Figure 9K**) in mouse HCC tissues.

In summary, TRAF3IP2-AS1 is downregulated by oxidative stress in HCC cells. The downstream miR-374a-5p is upregulated by downregulation of TRAF3IP2-AS1. MiR-374a-5p inhibits the expression of its target gene, SEL1L, an ERAD E3 ligase adaptor subunit. Consequently, the interaction between SEL1L and RPL6 decreases, resulting in a decrease in proteasome-dependent degradation of RPL6 and an increase in RPL6 expression. RPL6 promotes DDR inside HCC cells, thereby facilitating the proliferation, migration, and invasion of HCC cells (**Figure 10**).

Discussion

We first observed that TRAF3IP2-AS1 was downregulated by oxidative stress, while miR-374a-5p was upregulated in HCC. Furthermore, TRAF3IP2-AS1 inhibited the proliferation,

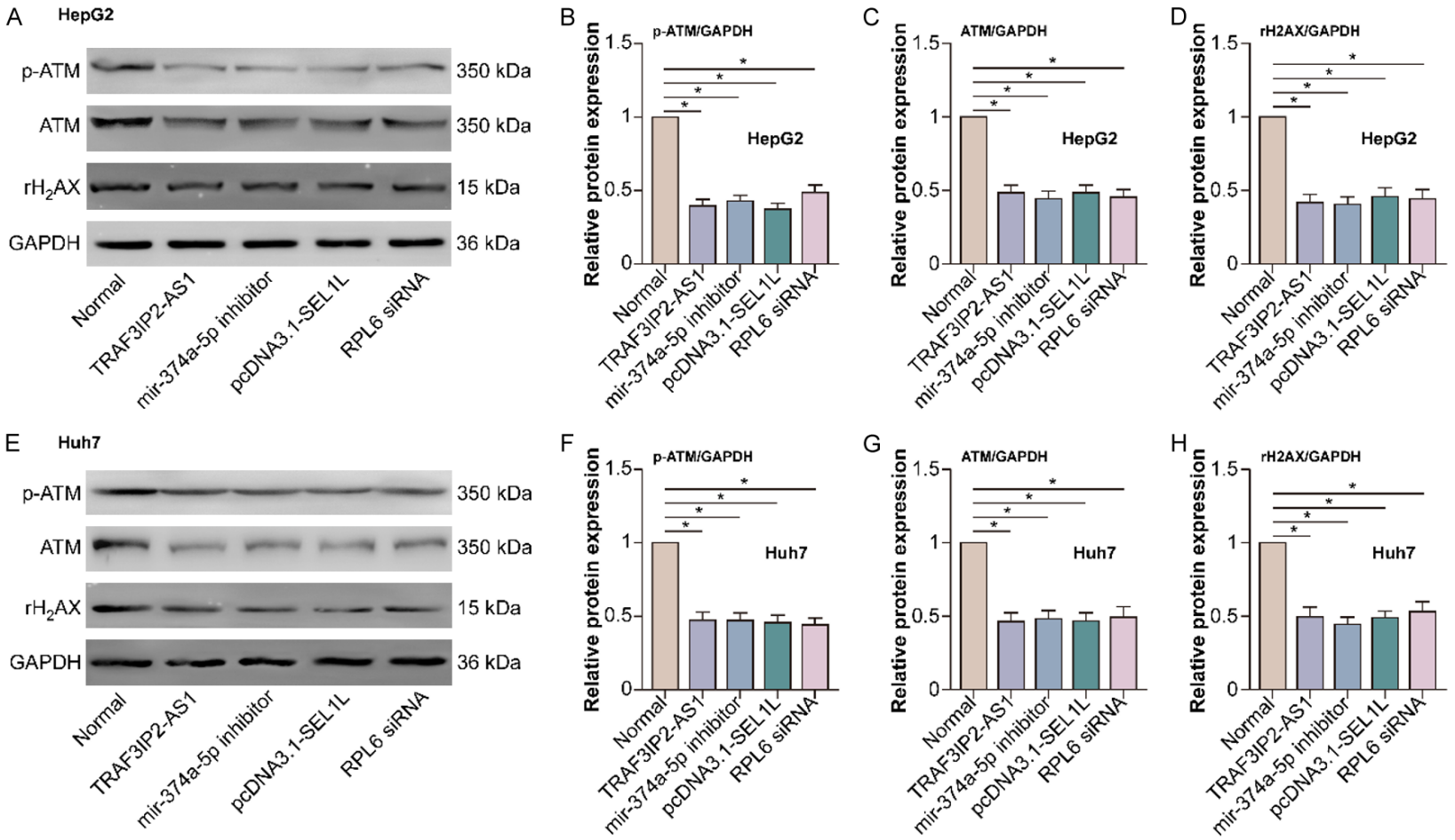

Figure 6. DNA damage repair (DDR) is upregulated in HCC cells by the TRAF3IP2-AS1/miR-374a-5p/SEL1L1/RPL6 pathway. HepG2 and Huh7 cells were divided into the normal, TRAF3IP2-AS1, miR-374a-5p inhibitor, pcDNA3.1-SEL1L, and RPL6 siRNA groups. (A) p-ataxia telangiectasia mutation (p-ATM) (S1981), ATM, and gamma H2A histone family member X (γH2AX) protein levels in HepG2 cells were evaluated through WB. (B-D) p-ATM, ATM, and γH2AX protein levels in HepG2 cells were analyzed. (E) p-ATM, ATM, and γH2AX protein levels in Huh7 cells were determined through WB. (F-H) p-ATM, ATM, and γH2AX protein levels in Huh7 cells were analyzed. In (B-D), $^{*}P < 0.05$ vs. the HepG2 cell normal group. In (F-H), $^{*}P < 0.05$ vs. the Huh7 cell normal group.

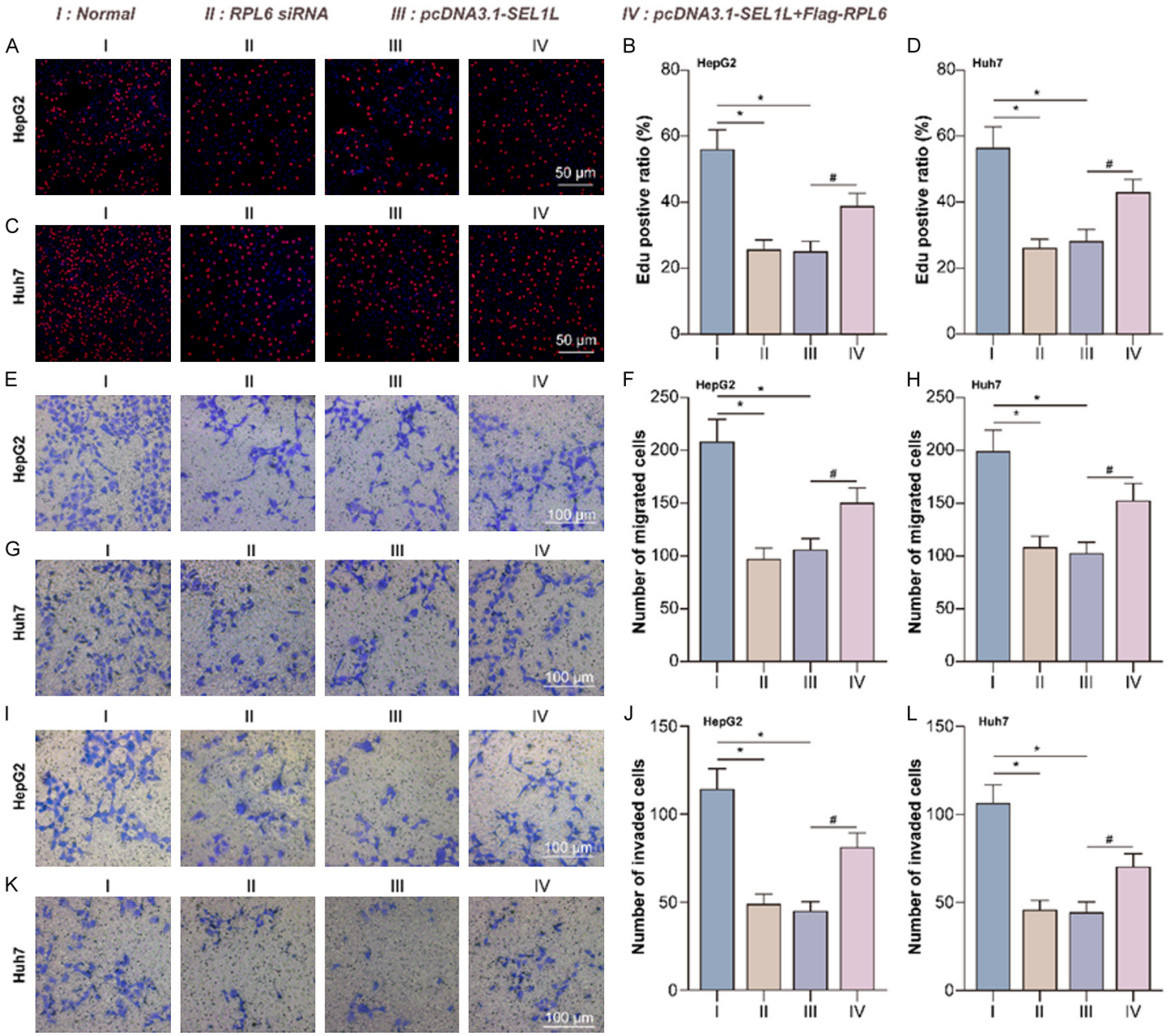
I : Normal
II : RPL6 siRNA
III : pcDNA3.1-SEL1L
IV : pcDNA3.1-SEL1L+Flag-RPL6
A
C
E
G
I
K
HepG2
Huh7
50 μm
100 μm
B
D
F
H
J
L
Edu postive ratio (%)
Number of migrated cells
Number of invaded cells
*
#

Figure 7. Downregulated SEL1L promotes the proliferation, migration, and invasion of HCC cells by upregulating RPL6 expression. HepG2 and Huh7 cells were divided into normal, RPL6 siRNA, pcDNA3.1-SEL1L, and pcDNA3.1-SEL1L + Flag-RPL6 groups. (A) HepG2 cell proliferation was detected using the EdU assay. (B) The ratio of EdU-positive HepG2 cells to DAPI-positive HepG2 cells was analyzed. (C) Huh7 cell proliferation was assessed using the EdU assay. (D) The ratio of EdU-positive Huh7 cells to DAPI-positive Huh7 cells was analyzed. (E) The migration of HepG2 cells was evaluated using the Transwell assay. (F) The number of migrated HepG2 cells was analyzed. (G) Migration of Huh7 cells was evaluated using the Transwell assay. (H) The number of migrated Huh7 cells was analyzed. (I) The invasion of HepG2 cells was determined through the Matrigel Transwell assay. (J) The number of invaded HepG2 cells was analyzed. (K) The invasion of Huh7 cells was assessed using the Matrigel Transwell assay. (L) The number of invaded Huh7 cells was analyzed. In (B, F, J), $^{*}P < 0.05$ vs. the HepG2 cell normal group. $^{\#}P < 0.05$ vs. the HepG2 cell pcDNA3.1-SEL1L group. In (D, H, L), $^{*}P < 0.05$ vs. the Huh7 cell normal group. $^{\#}P < 0.05$ vs. the Huh7 cell pcDNA3.1-SEL1L group.

migration, and invasion of HCC cells by downregulating miR-374a-5p levels. A previous study has found that under oxidative stress, lncRNAs, including AC091057.1 and SNHG5, are significantly downregulated in AGS and HGC-27 cells (two stomach adenocarcinoma cell lines) [26]. Similarly, we found that TRAF3IP2-AS1 was downregulated by oxidative stress in HCC cells. TRAF3IP2-AS1 acts as a tumor suppressor in multiple kinds of cancers, such as cervical cancer [27], glioblastoma multiforme [28], and pancreatic ductal adenocarcinoma [29], by sequestering downstream miRNAs or mRNA. These findings show the potential of TRAF3IP2-AS1 as a therapeutic target for cancers.

lncRNAs, which regulate oncogenic molecular networks in a cell type-restricted manner, have become a promising target for cancer therapy. lncRNAs differ from mRNAs and proteins in important aspects that both increase their value as therapeutic targets (for example, cell specificity, disease roles) but also present obstacles (for example, repetitiveness, rate of sequence evolution, and poor annotation) [30]. A hallmark of lncRNAs is their relatively high rate of sequence evolution compared with protein-coding genes, resulting in a lower rate of orthologue identification: only 16% of lncRNA genes have an orthologue between human and mouse, compared with 75% of protein-coding genes [31]. The lack of identifiable orthologues creates challenges in testing the disease roles and therapeutic perturbation of lncRNAs in genetically edited mouse models, which is commonly a vital step prior to clinical trials in humans. However, lncRNA structure is often more conserved than its primary sequence, raising the potential for small molecule inhibitors to target a conserved binding pocket [32].

miR-374a-5p promotes tumor progression in triple negative breast cancer [33] and gastric cancer [34]. SEL1L is a target gene of miR-374a-5p, and inhibits the progression of liver cancer, as evidenced by studies showing that hepatocyte-specific deletion of SEL1L predisposes mice to diet/chemical-induced tumors [13]. Additionally, SEL1L interference with SEL1L enhances valproic acid cytotoxic effects on glioma stem cells [35]. DDR contributes to the formation of HCC [36]. Interestingly, SEL1L interacts with RPL6, promoting the ubiquitination degradation of RPL6. RPL6 expression increases in HCC tissues and cells due to the decrease of SEL1L. RPL6 directly binds to histone H2A in response to DNA damage, and RPL6 silencing impairs DNA damage-induced H2A/H2AX ubiquitination, resulting in defects in DNA repair [16]. Our data also indicate that the increase of RPL6 mediated by downregulated SEL1L facilitates DDR in HCC cells.

In a mouse xenograft model of HepG2 cells, TRAF3IP2-AS1, miR-374a-5p, SEL1L, and RPL6 displayed similar changes as those observed in HCC cells. Moreover, TRAF3IP2-AS1 overexpression, miR-374a-5p knockdown, SEL1L overexpression, or RPL6 knockdown decreased liver tumor volume, weight, and mouse serum AFP levels, which extended the knowledge about the role of these molecules in HCC obtained from previous studies [6, 13, 37], suggesting effective strategies for interfering with HCC.

DNA damage is known to play an important role in the initiation of HCC, however the aberrant activation of DNA repair systems is also vital for the survival of HCC cells [38]. HCC is highly resistant to most classical chemotherapies, including those which work by inducing DNA damage, such as cisplatin [39]. The proposed DNA damage mechanism of HCC presents a tantalizing opportunity for targeted therapy towards HCC cells, due to an effect known as 'synthetic lethality'. When cancers arise due to deficiencies in DNA repair, and these pathways

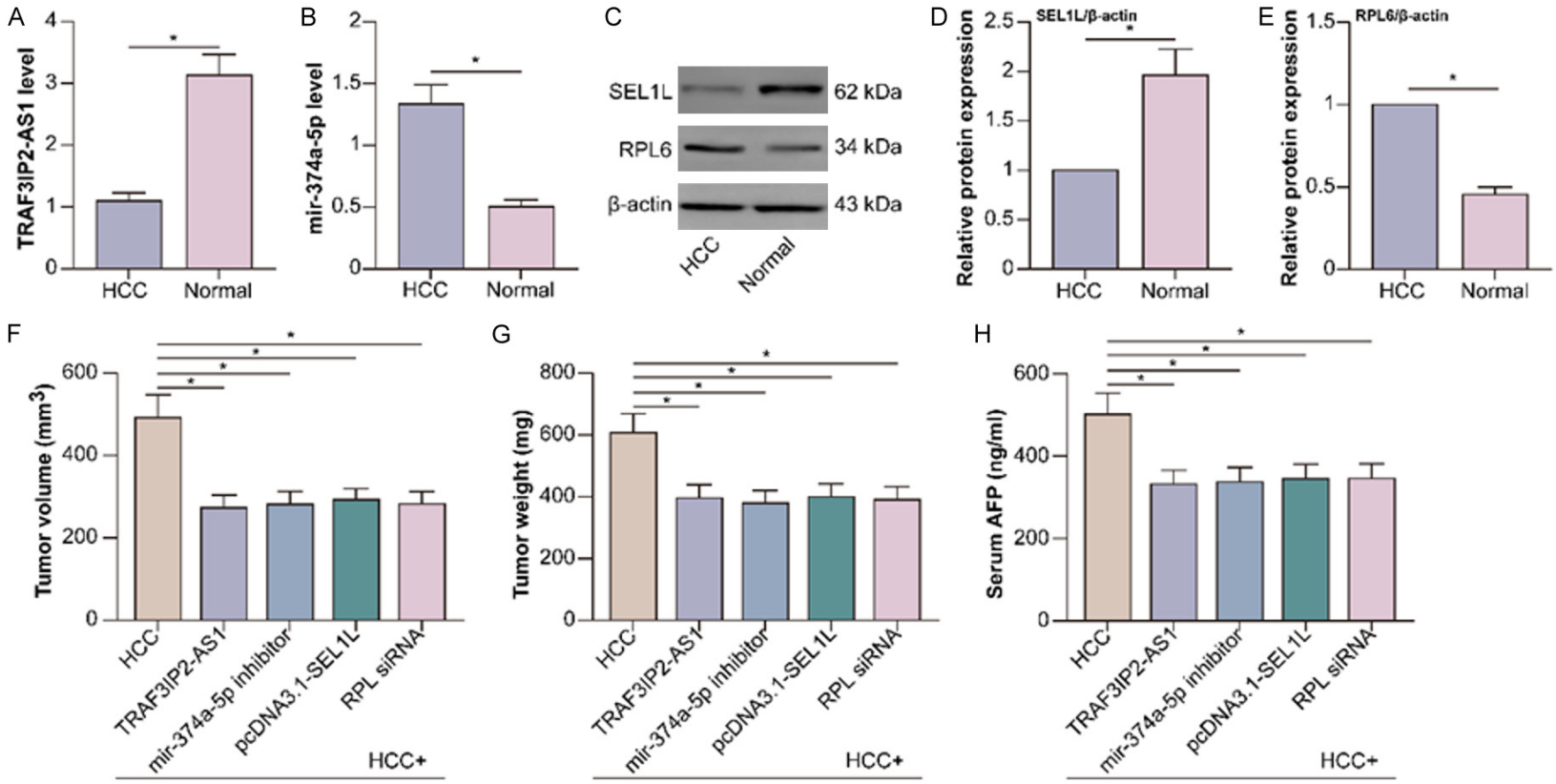

Figure 8. The TRAF3IP2-AS1/miR-374a-5p/SEL1L/RPL6 pathway exacerbates the progression of HCC in mice. (A) TRAF3IP2-AS1 levels in mouse HCC and adjacent tissues were evaluated through qRT-PCR. (B) Mir-374a-5p levels in mouse HCC and adjacent tissues were evaluated using qRT-PCR. (C) SEL1L and RPL6 protein levels in mouse HCC and adjacent tissues were assessed using WB. (D, E) SEL1L and RPL6 protein levels were analyzed. The mice were divided into HCC, HCC + TRAF3IP2-AS1, HCC + miR-374a-5p inhibitor, HCC + pcDNA3.1-SEL1L, and HCC + RPL6 siRNA steady transfection groups. (F) The volume of HCC tissue was measured and calculated. (G) The weight of HCC tissue was measured. (H) AFP in mouse serum was detected using ELISA. In (A, B, D, E), $^{*}P < 0.05$ vs. the normal liver tissue group. In (F-H), $^{*}P < 0.05$ vs. the HCC group.

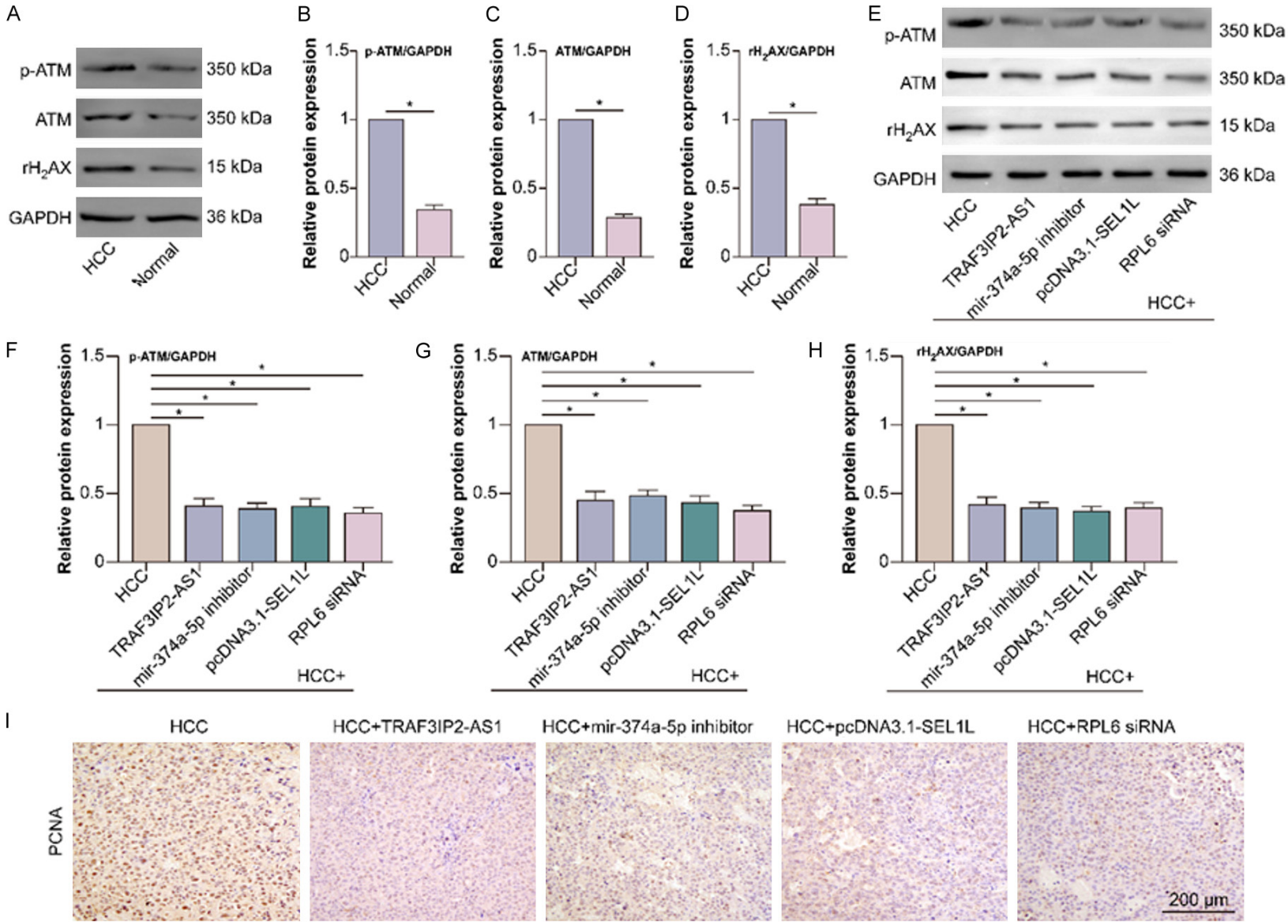
A
p-ATM
ATM
rH2AX
GAPDH
350 kDa
350 kDa
15 kDa
36 kDa
HCC
Normal
B
p-ATM/GAPDH
Relative protein expression
C
ATM/GAPDH
D
rH2AX/GAPDH
E
TRAF3IP2-AS1
mir-374a-5p inhibitor
pcDNA3.1-SEL1L
RPL6 siRNA
HCC+
F
G
H
I
HCC
HCC+TRAF3IP2-AS1
HCC+mir-374a-5p inhibitor
HCC+pcDNA3.1-SEL1L
HCC+RPL6 siRNA
PCNA
200 μm

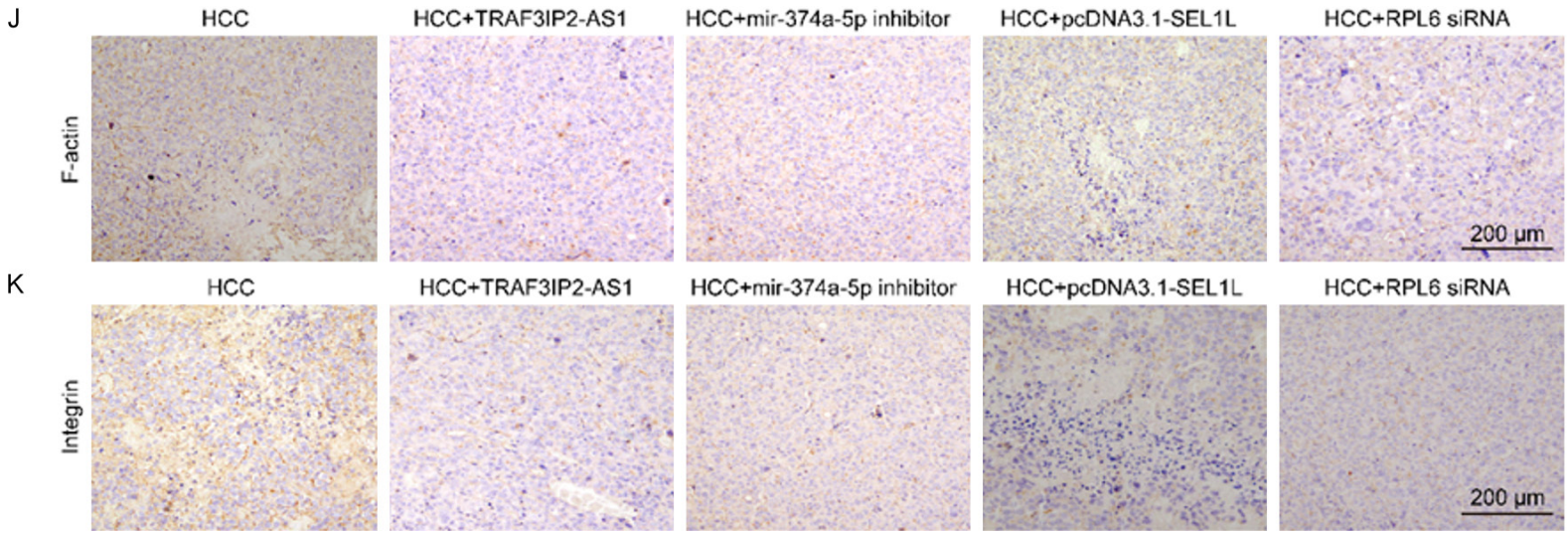

Figure 9. The TRAF3IP2-AS1/miR-374a-5p/SEL1L/RPL6 pathway promotes the proliferation, migration, and invasion of *in vivo* HCC cells by enhancing DDR. (A) p-ATM, ATM, and γH2AX protein levels in mouse HCC and adjacent tissues were evaluated using WB. (B-D) p-ATM, ATM, and γH2AX protein levels were analyzed. The mice were divided into HCC, HCC + TRAF3IP2-AS1, HCC + miR-374a-5p inhibitor, HCC + pcDNA3.1-SEL1L, and HCC + RPL6 siRNA steady transfection groups. (E) p-ATM, ATM, and γH2AX protein levels in mouse HCC tissues were evaluated using WB. (F-H) Analysis of p-ATM, ATM, and γH2AX protein levels. (I-K) PCNA, F-actin and β1-integrin in mouse HCC tissue were detected using IHC. In (B-D), $^{*}P < 0.05$ vs. normal liver tissue group. In (F-H), $^{*}P < 0.05$ vs. the HCC group.

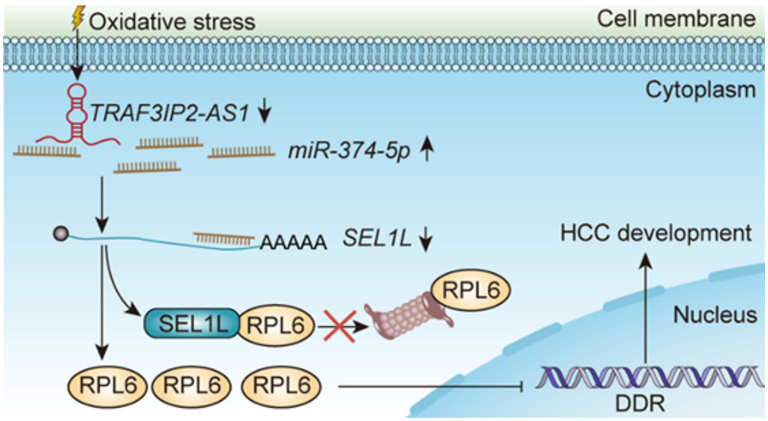

Figure 10. Illustration of the TRAF3IP2-AS1/miR-374a-5p/SEL1L/RPL6 pathway in HCC. In HCC cells, TRAF3IP2-AS1 is downregulated by oxidative stress. The downstream miR-374a-5p is upregulated by downregulated TRAF3IP2-AS1. Subsequently, miR-374a-5p inhibits the expression of its target gene ERAD E3 ligase adaptor subunit SEL1L. A decreased interaction between SEL1L and RPL6 leads to a reduction in proteasome-dependent degradation of RPL6 and an increase in RPL6 expression. RPL6 promotes DDR inside HCC cells, consequently facilitating the proliferation, migration, and invasion of HCC cells.

are recovered by other redundant repair pathways, they become highly sensitive to therapeutics targeting those repair pathways. This means that pharmacological inhibitors are synthetically lethal to these cancer cells, while they have little effect on functionally normal cells [40]. Furthermore, evidence suggests that while most cancer types tend to have co-occurrence of mutations in DNA-repair enzymes, liver cancer is unique in that DNA-repair mutations are generally mutually exclusive [41]. This suggests that loss of multiple DNA repair pathways is particularly detrimental to HCC, meaning that they would be hypersensitive to synthetically lethal drugs. DDR is upregulated in a mouse xenograft model of HepG2 cells, whereas TRAF3IP2-AS1 overexpression, miR-374a-5p knockdown, SEL1L overexpression, or RPL6 knockdown inhibits DDR. A previous study revealed that TRAF3IP2-AS1 is associated with DDR of diffuse large B-cell lymphoma (DLBCL), although the specific role and mechanism were not elucidated [42]. Our study sheds new light on the role and mechanism of TRAF3IP2-AS1 in DDR. As far as we know, the role of miR-374a-5p during DDR is obscure, but our study suggests that miR-374a-5p promotes DDR during the progression of HCC. Presently, the role of SEL1L in DDR is unclear. Our study reveals a negative regulatory function of SEL1L in DDR, extending its biological function. Additionally, our investigation demonstrates the positive regulatory role of RPL6 in DDR [16]. In studies, PCNA, F-actin, and β1-integrin were used as markers of HCC cell proliferation [43], migration [44], and invasion [45] to identify TRAF3IP2-AS1 overexpression, knockdown, SEL1L overexpression, or RPL6 knockdown inhibition effects on *in vivo* HepG2 cell tumor behavior.

Conclusion

Our study showed that the TRAF3IP2-AS1/miR-374a-5p/SEL1L/RPL6 pathway in HCC cells promotes DDR and HCC progression. Admittedly, we have not used the DDR inhibitor to confirm the role of DDR in HCC. In addition, the lung metastasis of HepG2 cells has not been assessed using an *in vivo* imaging system, which is our future research direction. Despite these limitations of our study, our data suggest that the TRAF3IP2-AS1/miR-374a-5p/SEL1L/RPL6 pathway plays a vital function in the progression of HCC and may be a treatment option for HCC.

Acknowledgements

This work was supported by Funding Medical Education Collaborative Innovation Fund of Jiangsu University (No. JDY2022018), Changzhou Science and Technology Program Grant No. CJ20210006, the Clinical Medical Science and Technology Development Fund of Jiangsu University (No. JLY2021095), and the School-based education and teaching research project of Jiangsu Vocational College of Medicine (No. Z202304).

Disclosure of conflict of interest

None.

Address correspondence to: Dong-Lin Sun, Department of Hepatobiliary Surgery, The Third Affiliated Hospital of Soochow University, Changzhou 213003, Jiangsu, China. Tel: +86-0519-68870000; E-mail: czyysdl@163.com

References

[1] Sung H, Ferlay J, Siegel RL, Laversanne M, Soerjomataram I, Jemal A and Bray F. Global cancer statistics 2020: GLOBOCAN estimates of incidence and mortality worldwide for 36 cancers in 185 countries. CA Cancer J Clin 2021; 71: 209-249.

[2] Llovet JM, Kelley RK, Villanueva A, Singal AG, Pikarsky E, Roayaie S, Lencioni R, Koike K, Zucman-Rossi J and Finn RS. Hepatocellular carcinoma. Nat Rev Dis Primers 2021; 7: 6.

[3] Wang C, Tang H, Geng A, Dai B, Zhang H, Sun X, Chen Y, Qiao Z, Zhu H, Yang J, Chen J, He Q, Qin N, Xie J, Tan R, Wan X, Gao S, Jiang Y, Sun FL and Mao Z. Rational combination therapy for hepatocellular carcinoma with PARP1 and DNA-PK inhibitors. Proc Natl Acad Sci U S A 2020; 117: 26356-26365.

[4] Han D, Li J, Wang H, Su X, Hou J, Gu Y, Qian C, Lin Y, Liu X, Huang M, Li N, Zhou W, Yu Y and Cao X. Circular RNA circMTO1 acts as the sponge of microRNA-9 to suppress hepatocellular carcinoma progression. Hepatology 2017; 66: 1151-1164.

[5] Hua S, Lei L, Deng L, Weng X, Liu C, Qi X, Wang S, Zhang D, Zou X, Cao C, Liu L and Wu D. miR-139-5p inhibits aerobic glycolysis, cell proliferation, migration, and invasion in hepatocellular carcinoma via a reciprocal regulatory interaction with ETS1. Oncogene 2018; 37: 1624-1636.

[6] Yang L, Chen Y, Liu N, Shi Q, Han X, Gan W and Li D. Low expression of TRAF3IP2-AS1 promotes progression of NONO-TFE3 translocation renal cell carcinoma by stimulating N(6)-methyladenosine of PARP1 mRNA and downregulating PTEN. J Hematol Oncol 2021; 14: 46.

[7] He R, Wu S, Gao R, Chen J, Peng Q, Hu H, Zhu L, Du Y, Sun W, Ma X, Zhang H, Cui Z, Wang H, Martin BN, Wang Y, Zhang CJ and Wang C. Identification of a long noncoding RNA TRAF3IP2-AS1 as key regulator of IL-17 signaling through the SRSF10-IRF1-Act1 axis in autoimmune diseases. J Immunol 2021; 206: 2353-2365.

[8] Wang J, Li J, Wu J, Dong M, Shen Z, Lin Y, Li F, Zhang Y, Mao R, Lu M and Zhang J. Host gene SEL1L involved in endoplasmic reticulum-associated degradation pathway could inhibit hepatitis B virus at RNA, DNA, and protein levels. Front Microbiol 2019; 10: 2869.

[9] Mangalaparthi KK, Patel K, Khan AA, Nair B, Kumar RV, Prasad TSK, Sidransky D, Chatterjee A, Pandey A and Gowda H. Molecular characterization of esophageal squamous cell carcinoma using quantitative proteomics. Cancers (Basel) 2023; 15: 3302.

[10] Niemira M, Collin F, Szalkowska A, Bielska A, Chwialkowska K, Reszec J, Niklinski J, Kwasniewski M and Kretowski A. Molecular signature of subtypes of non-small-cell lung cancer by large-scale transcriptional profiling: identification of key modules and genes by weighted gene co-expression network analysis (WGCNA). Cancers (Basel) 2019; 12: 37.

[11] Ping D, Pu X, Ding G, Zhang C, Jin J, Xu C, Liu J, Jia S and Cao L. Sirtuin4 impacts mitochondrial homeostasis in pancreatic cancer cells by reducing the stability of AlkB homolog 1 via deacetylation of the HRD1-SEL1L complex. Biochim Biophys Acta Gene Regul Mech 2023; 1866: 194941.

[12] Song Z, Thepsuwan P, Hur WS, Torres M, Wu SA, Wei X, Tushi NJ, Wei J, Ferraresso F, Paton AW, Paton JC, Zheng Z, Zhang K, Fang D, Kastrup CJ, Jaiman S, Flick MJ and Sun S. Regulation of hepatic inclusions and fibrinogen biogenesis by SEL1L-HRD1 ERAD. Nat Commun 2024; 15: 9244.

[13] Bhattacharya A, Wei J, Song W, Gao B, Tian C, Wu SA, Wang J, Chen L, Fang D and Qi L. SEL1L-HRD1 ER-associated degradation suppresses hepatocyte hyperproliferation and liver cancer. iScience 2022; 25: 105183.

[14] Mellai M, Annovazzi L, Boldorini R, Bertero L, Cassoni P, De Blasio P, Biunno I and Schiffer D. SEL1L plays a major role in human malignant gliomas. J Pathol Clin Res 2020; 6: 17-29.

[15] Shigeno Y, Uchiumi T and Nomura T. Involvement of ribosomal protein L6 in assembly of functional 50S ribosomal subunit in Escherichia coli cells. Biochem Biophys Res Commun 2016; 473: 237-242.

[16] Yang C, Zang W, Ji Y, Li T, Yang Y and Zheng X. Ribosomal protein L6 (RPL6) is recruited to DNA damage sites in a poly(ADP-ribose) polymerase-dependent manner and regulates the DNA damage response. J Biol Chem 2019; 294: 2827-2838.

[17] Zhang J, Ma Q, Han Y, Wen H, Zhang Z, Hao Y, Xiao F and Liang C. Downregulated RPL6 inhibits lung cancer cell proliferation and migration and promotes cell apoptosis by regulating the AKT signaling pathway. J Thorac Dis 2022; 14: 507-514.

[18] Wu Q, Gou Y, Wang Q, Jin H, Cui L, Zhang Y, He L, Wang J, Nie Y, Shi Y and Fan D. Downregulation of RPL6 by siRNA inhibits proliferation and cell cycle progression of human gastric cancer cell lines. PLoS One 2011; 6: e26401.

[19] Gao Y, Wang Z, Zhu Y, Zhu Q, Yang Y, Jin Y, Zhang F, Jiang L, Ye Y, Li H, Zhang Y, Liang H, Xiang S, Miao H, Liu Y and Hao Y. NOP2/Sun RNA methyltransferase 2 promotes tumor progression via its interacting partner RPL6 in gallbladder carcinoma. Cancer Sci 2019; 110: 3510-3519.

[20] Guo Q, Wang H, Xu Y, Wang M and Tian Z. miR-374a-5p inhibits non-small cell lung cancer cell proliferation and migration via targeting NCK1. Exp Ther Med 2021; 22: 943.
[21] Wang P, Wang M, Hu Y, Chen J, Cao Y, Liu C, Wu Z, Shen J, Lu J and Liu P. Isorhapontigenin protects against doxorubicin-induced cardiotoxicity via increasing YAP1 expression. Acta Pharm Sin B 2021; 11: 680-693.
[22] Wang Z, Sun P, Pan B, Qiu J, Zhang X, Shen S, Ke X and Tang N. IL-33/ST2 antagonizes STING signal transduction via autophagy in response to acetaminophen-mediated toxicological immunity. Cell Commun Signal 2023; 21: 80.
[23] McLoughlin MR, Orlicky DJ, Prigge JR, Krishna P, Talago EA, Cavigli IR, Eriksson S, Miller CG, Kundert JA, Sayin VI, Sabol RA, Heinemann J, Brandenberger LO, Iverson SV, Bothner B, Papagiannakopoulos T, Shearn CT, Arnér ESJ and Schmidt EE. TrxR1, Gsr, and oxidative stress determine hepatocellular carcinoma malignancy. Proc Natl Acad Sci U S A 2019; 116: 11408-11417.
[24] Wu L, Pan C, Wei X, Shi Y, Zheng J, Lin X and Shi L. lncRNA KRAL reverses 5-fluorouracil resistance in hepatocellular carcinoma cells by acting as a ceRNA against miR-141. Cell Commun Signal 2018; 16: 47.
[25] Horn S, Brady D and Prise K. Alpha particles induce pan-nuclear phosphorylation of H2AX in primary human lymphocytes mediated through ATM. Biochim Biophys Acta 2015; 1853: 2199-2206.
[26] Zhang H, Feng H, Yu T, Zhang M, Liu Z, Ma L and Liu H. Construction of an oxidative stress-related lncRNAs signature to predict prognosis and the immune response in gastric cancer. Sci Rep 2023; 13: 8822.
[27] Luo C and Pang X. lncRNA TRAF3IP2-AS1 restrains cervical cancer progression by sponging miR-3677-3p and acts as a diagnostic marker in cervical cancer. Crit Rev Eukaryot Gene Expr 2022; 33: 43-51.
[28] Alt EU, Barabadi Z, Pfnür A, Ochoa JE, Daneshimehr F, Lang LM, Lin D, Braun SE, Chandrasekar B and Izadpanah R. TRAF3IP2, a novel therapeutic target in glioblastoma multiforme. Oncotarget 2018; 9: 29772-29788.
[29] Xu G, Ji Y, Wang L, Xu H, Shen C, Ye H and Yang X. M6A-related long non-coding RNA displays utility in predicting prognosis, portraying the tumor immune microenvironment and guiding immunotherapy in pancreatic ductal adenocarcinoma. Vaccines (Basel) 2023; 11: 499.
[30] Coan M, Haefliger S, Ounzain S and Johnson R. Targeting and engineering long non-coding RNAs for cancer therapy. Nat Rev Genet 2024; 25: 578-595.
[31] Chen J, Shishkin AA, Zhu X, Kadri S, Maza I, Guttman M, Hanna JH, Regev A and Garber M. Evolutionary analysis across mammals reveals distinct classes of long non-coding RNAs. Genome Biol 2016; 17: 19.
[32] Rivas E. Evolutionary conservation of RNA sequence and structure. Wiley Interdiscip Rev RNA 2021; 12: e1649.
[33] Son D, Kim Y, Lim S, Kang HG, Kim DH, Park JW, Cheong W, Kong HK, Han W, Park WY, Chun KH and Park JH. miR-374a-5p promotes tumor progression by targeting ARRB1 in triple negative breast cancer. Cancer Lett 2019; 454: 224-233.
[34] Ji R, Zhang X, Gu H, Ma J, Wen X, Zhou J, Qian H, Xu W, Qian J and Lin J. miR-374a-5p: a new target for diagnosis and drug resistance therapy in gastric cancer. Mol Ther Nucleic Acids 2019; 18: 320-331.
[35] Cattaneo M, Baronchelli S, Schiffer D, Mellai M, Caldera V, Saccani GJ, Dalpra L, Daga A, Orlandi R, DeBlasio P and Biunno I. Down-modulation of SEL1L, an unfolded protein response and endoplasmic reticulum-associated degradation protein, sensitizes glioma stem cells to the cytotoxic effect of valproic acid. J Biol Chem 2014; 289: 2826-2838.
[36] Kumar D, Das M, Oberg A, Sahoo D, Wu P, Sauceda C, Jih L, Ellies LG, Langiewicz MT, Sen S and Webster NJG. Hepatocyte deletion of IGF2 prevents DNA damage and tumor formation in hepatocellular carcinoma. Adv Sci (Weinh) 2022; 9: e2105120.
[37] Wang C, Su K, Lin H, Cen B, Zheng S and Xu X. Identification and verification of a novel MAGI2-AS3/miRNA-374-5p/FOXO1 network associated with HBV-related HCC. Cells 2022; 11: 3466.
[38] Gillman R, Lopes Floro K, Wankell M and Hebbard L. The role of DNA damage and repair in liver cancer. Biochim Biophys Acta Rev Cancer 2021; 1875: 188493.
[39] Zeng Y, Jiang H, Zhang X, Xu J, Wu X, Xu Q, Cai W, Ying H, Zhou R, Ding Y, Ying K, Song X, Chen Z, Zeng L, Zhao L and Yu F. Canagliflozin reduces chemoresistance in hepatocellular carcinoma through PKM2-c-Myc complex-mediated glutamine starvation. Free Radic Biol Med 2023; 208: 571-586.
[40] Aubert L, Bastien E, Renoult O, Guilbaud C, Özkan K, Brusa D, Bouzin C, Richiardone E, Richard C, Boidot R, Léonard D, Corbet C and Feron O. Tumor acidosis-induced DNA damage response and tetraploidy enhance sensitivity to ATM and ATR inhibitors. EMBO Rep 2024; 25: 1469-1489.
[41] Groelly FJ, Fawkes M, Dagg RA, Blackford AN and Tarsounas M. Targeting DNA damage re-

sponse pathways in cancer. Nat Rev Cancer 2023; 23: 78-94.
[42] Li Y, Liu X, Chang Y, Fan B, Shangguan C, Chen H and Zhang L. Identification and validation of a DNA damage repair-related Signature for diffuse large B-cell lymphoma. Biomed Res Int 2022; 2022: 2645090.
[43] Li DD, Zhang JW, Zhang R, Xie JH, Zhang K, Lin GG, Han YX, Peng RX, Han DS, Wang J, Yang J and Li JM. Proliferating cell nuclear antigen (PCNA) overexpression in hepatocellular carcinoma predicts poor prognosis as determined by bioinformatic analysis. Chin Med J (Engl) 2020; 134: 848-850.
[44] Zhang L, Chai Z, Kong S, Feng J, Wu M, Tan J, Yuan M, Chen G, Li Z, Zhou H, Cheng S and Xu H. Nujiangexanthone a inhibits hepatocellular carcinoma metastasis via down regulation of cofilin 1. Front Cell Dev Biol 2021; 9: 644716.
[45] Meder L, Orschel CI, Otto CJ, Koker M, Brägelmann J, Ercanoglu MS, Dähling S, Compes A, Selenz C, Nill M, Dietlein F, Florin A, Eich ML, Borchmann S, Odenthal M, Blazquez R, Hilberg F, Klein F, Hallek M, Büttner R, Reinhardt HC and Ullrich RT. Blocking the angiopoietin-2-dependent integrin β-1 signaling axis abrogates small cell lung cancer invasion and metastasis. JCI Insight 2024; 9: e166402.

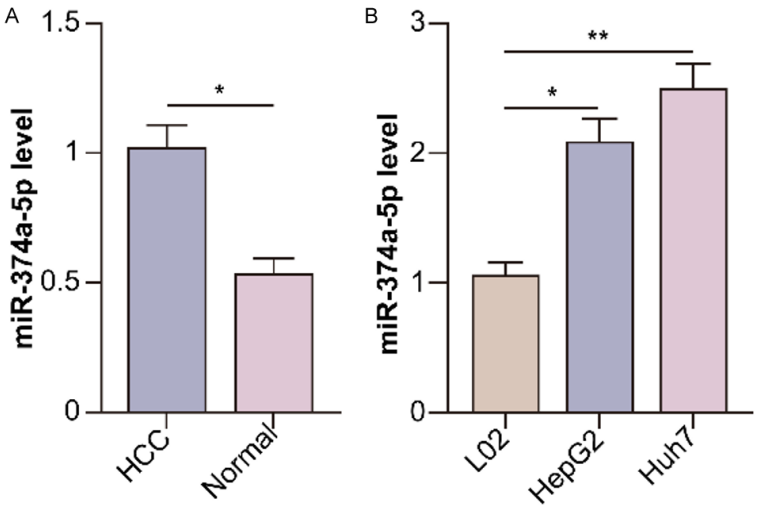

Figure S1. MiR-374a-5p increases in human HCC tissues and cells. A: MiR-374a-5p levels in human HCC and adjacent tissues were determined through qRT-PCR. $^{*}P < 0.05$ vs. the normal liver tissue group. B: MiR-374a-5p levels in L02, HepG2, and Huh7 cells were determined through qRT-PCR. $^{*}P < 0.05$, $^{**}P < 0.01$ vs. the L02 cell group.

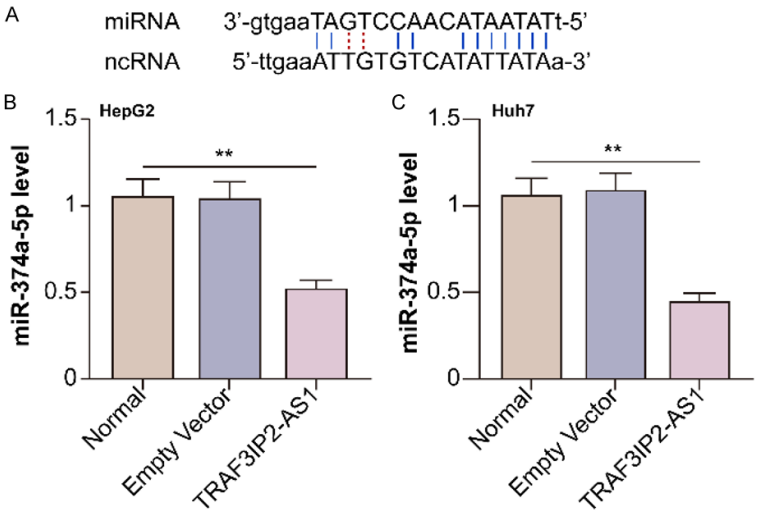

Figure S2. TRAF3IP2-AS1 downregulates miR-374a-5p in HCC cells. A: The binding site between miR-374a-5p and TRAF3IP2-AS1 is shown. HepG2 and Huh7 cells were divided into normal, empty vector, and TRAF3IP2-AS1 groups. B: Mir-374a-5p levels in HepG2 cells were determined through qRT-PCR. $^{**}P < 0.01$ vs. the HepG2 cell normal group. C: MiR-374a-5p levels in Huh7 cells were evaluated through qRT-PCR. $^{**}P < 0.01$ vs. the Huh7 cell normal group.

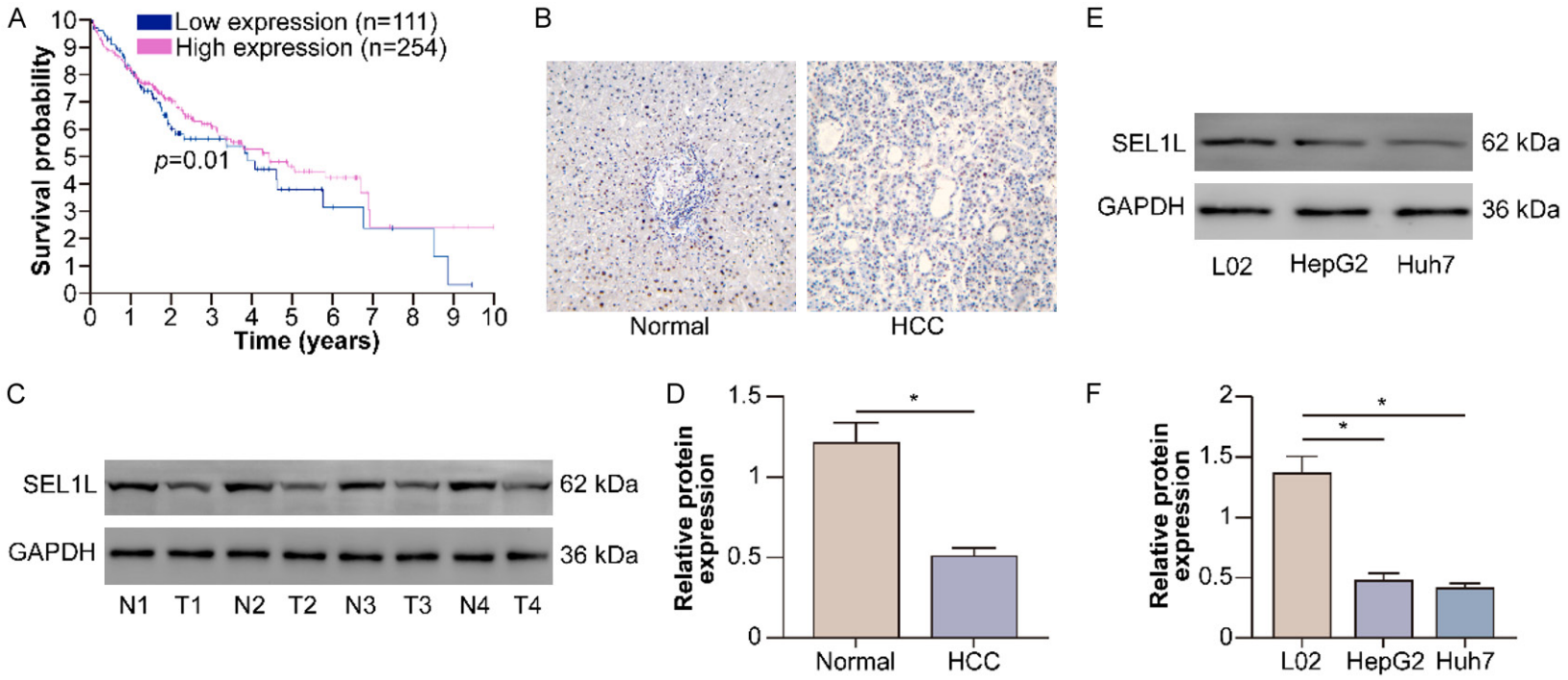

Figure S3. SEL1L is decreased in human HCC tissues and cells, which positively correlates with a poor prognosis in HCC patients. A: The negative correlation between SEL1L and the overall survival of HCC patients from TCGA is shown. B: SEL1L expression in human HCC and adjacent tissues was determined through IHC. C: SEL1L protein levels in human HCC and adjacent tissues were evaluated through WB. D: SEL1L relative protein levels were analyzed. $^{*}P < 0.05$ vs. the normal liver tissue group. E: SEL1L protein levels in L02, HepG2, and Huh7 cells were determined through WB analysis. F: SEL1L relative protein levels were analyzed. $^{*}P < 0.05$ vs. the L02 cell group.

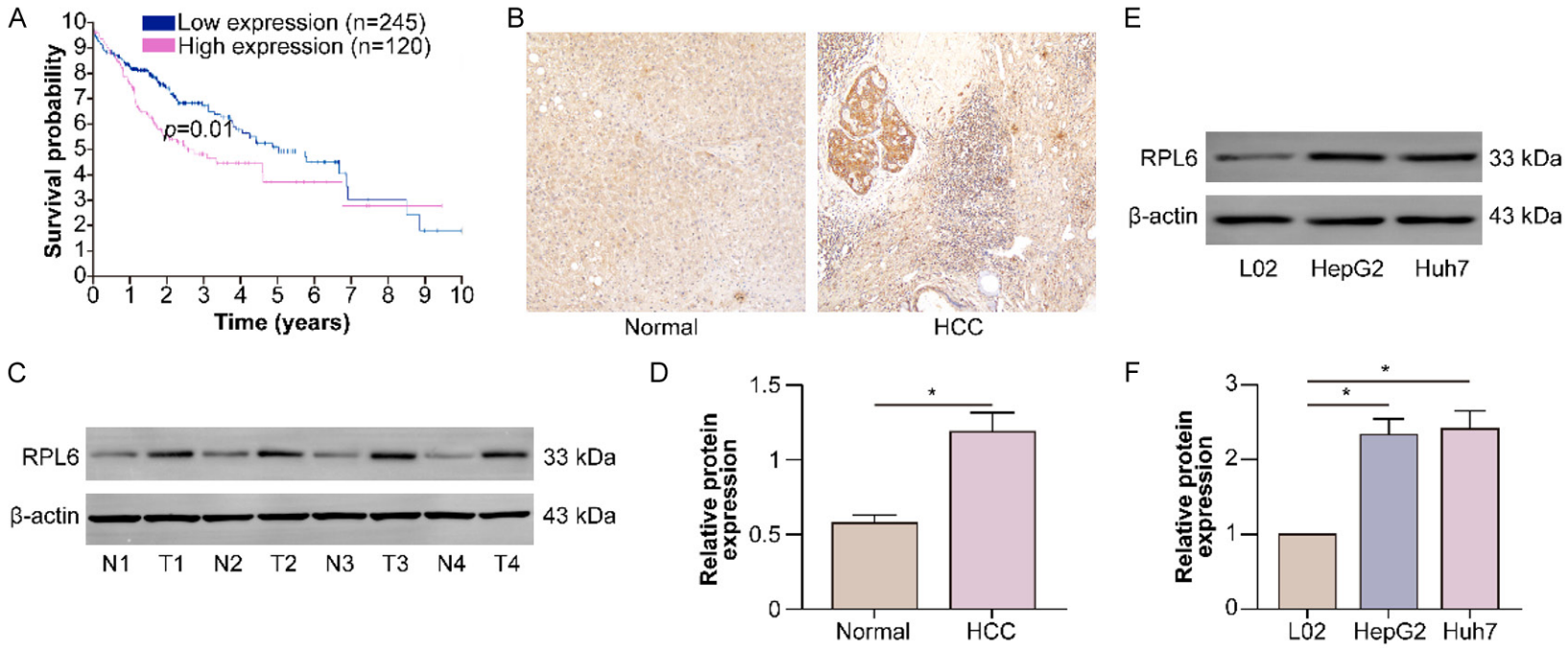

Figure S4. RPL6 is decreased in human HCC tissues and cells, which is positively correlated with a poor prognosis in HCC patients. A: Negative correlation between RPL6 and the overall survival of HCC patients from TCGA is shown. B: RPL6 expression in human HCC and adjacent tissues was evaluated using IHC. C: RPL6 protein levels in human HCC and adjacent tissues were determined through WB. D: RPL6 relative protein levels were analyzed. $^{*}P < 0.05$ vs. the normal liver tissue group. E: RPL6 protein levels in L02, HepG2, and Huh7 cells were determined through WB. F: RPL6 relative protein levels were analyzed. $^{*}P < 0.05$ vs. the L02 cell group.

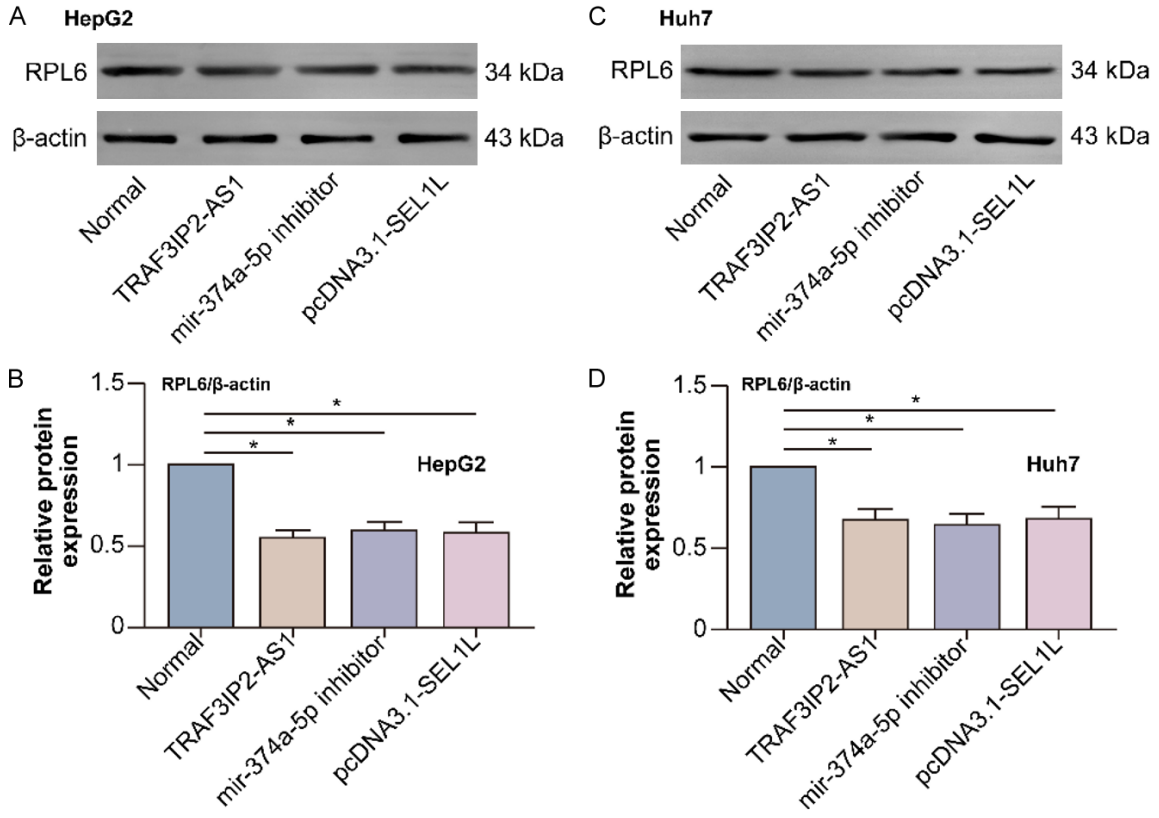

Figure S5. RPL6 in HCC cells is upregulated by the TRAF3IP2-AS1/miR-374a-5p/SEL1L pathway. HepG2 and Huh7 cells were divided into normal, TRAF3IP2-AS1, miR-374a-5p inhibitor, and SEL1L plasmid groups. A: RPL6 protein levels in HepG2 cells were determined through WB. B: RPL6 protein levels in HepG2 cells were analyzed. $^{*}P < 0.05$ vs. the HepG2 cell normal group. C: RPL6 protein levels in Huh7 cells were evaluated through WB. D: RPL6 protein levels in Huh7 cells were analyzed. $^{*}P < 0.05$ vs. the Huh7 cell normal group.

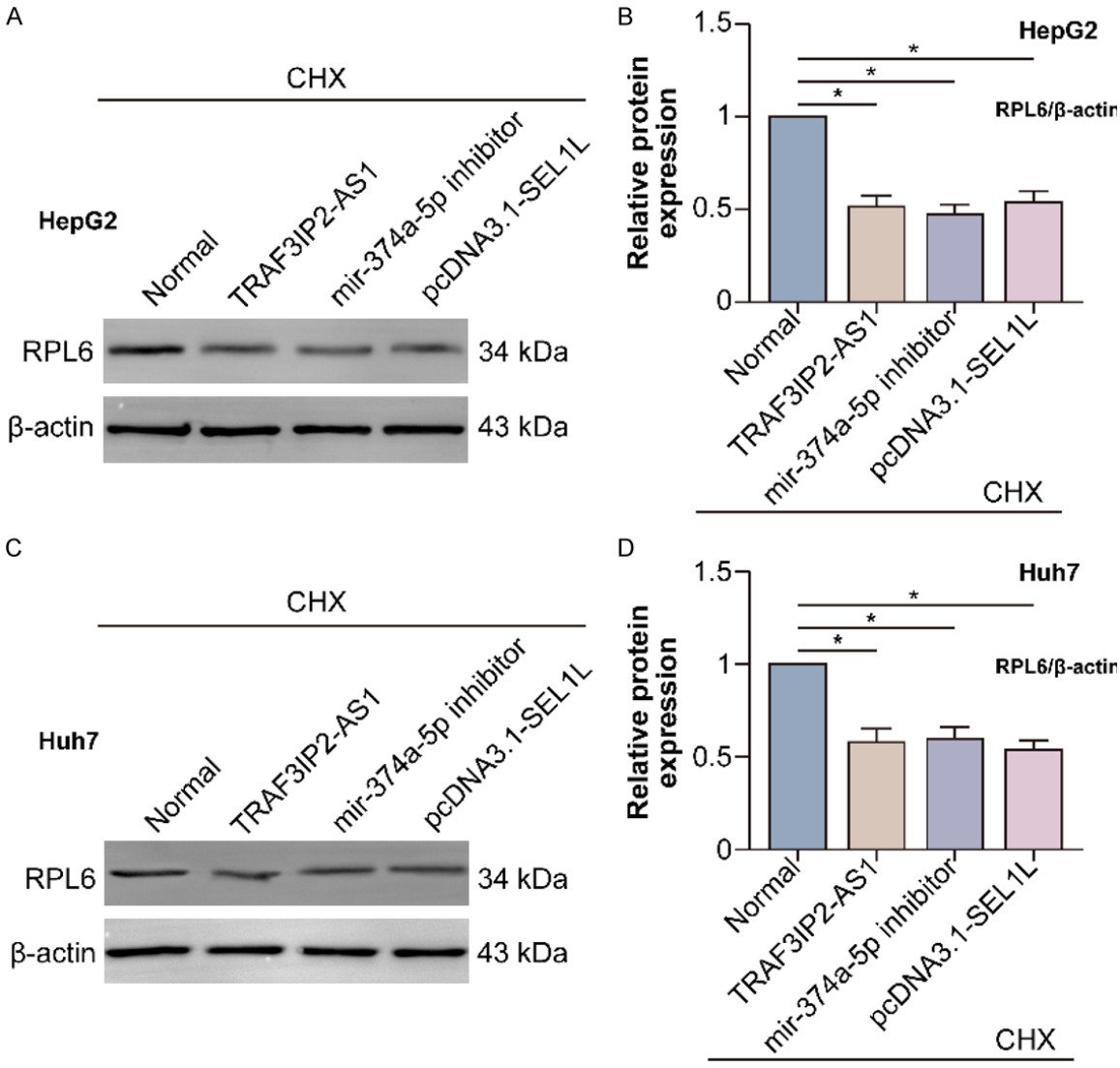

Figure S6. The half-life of RPL6 is upregulated by the TRAF3IP2-AS1/miR-374a-5p/SEL1L1 pathway in human HCC cells. HepG2 and Huh7 cells were divided into CHX (20 pg/ml for 24 h), CHX + TRAF3IP2-AS1 (transfection for 24 h), CHX + miR-374a-5p inhibitor (transfection for 24 h), and CHX + pcDNA3.1-SEL1L (transfection for 24 h) groups. A: RPL6 protein levels in HepG2 cells were determined through WB. B: RPL6 protein levels in HepG2 cells were analyzed. $^{*}P < 0.05$ vs. the HepG2 cell normal group. C: RPL6 protein levels in Huh7 cells were determined through WB. D: RPL6 protein levels in Huh7 cells were analyzed. $^{*}P < 0.05$ vs. the Huh7 cell normal group.